Groundwater Pumping Decisions and Land Subsidence in the Southern Chesapeake Bay Region of Virginia

Christopher Michael Wade

Thesis submitted to the faculty of the Virginia Polytechnic Institute and State University in partial fulfillment of the requirements for the degree of

Master of Science
In
Forest Resources and Environmental Conservation

Kelly Cobourn
Jay Sullivan
Greg Amacher
Erich Hester

May 16th, 2016
Blacksburg, Virginia

Keywords: Groundwater, spatial externality, land subsidence

Groundwater Pumping Decisions and Land Subsidence in the Southern Chesapeake Bay Region of Virginia

Christopher Michael Wade

ABSTRACT

Land subsidence is the gradual settling or sudden sinking of the earth's surface. According to the United States Geological Survey more than 80% of identified subsidence in the United States is a result of groundwater removal. Due to the hydrologic structure and reliance on the Potomac Aquifer, the Southern Chesapeake Bay region of Virginia has suffered from land subsidence since the 1940s. In coastal regions, land subsidence can increase the risk of flooding. This paper presents a mathematical simulation that predicts land subsidence from groundwater pumping. This simulation is used to see how the location of groundwater pumping, as well as the amount of amount of groundwater pumped would differ from two different groundwater pumping policies. The first policy is aimed at limiting land subsidence in the region, while the second policy aims at limiting the damages from land subsidence. These two policies are used to show that a spatially heterogeneous groundwater pumping policy is necessary to minimize the damages from groundwater pumping when land subsidence is present.

Acknowledgments

I want to begin by thanking my beautiful fiancé, Rachael, for supporting me throughout this entire process. Your love and support has truly propelled me through this process and I am happy to say that these two years have brought us even closer together. Next, I need to thank my Advisor, Dr. Kelly Cobourn. You continually pushed me to be the best student that I could be and through this process have shown me that I can succeed at any task to which I fully commit. I also need to thank all the professors that I have had here at Virginia Tech as well as the professors I had at UNC-Wilmington who helped shape my interest in economics. Lastly, I need to give a shout out to all the friends that I have made over these past two years. I couldn't have asked for a better group of people to share all of the challenges and successes that come with graduate school.

Table of Contents

List of Tables

List of Figures

CHAPTER 1. INTRODUCTION

According to the United States Geological Survey (USGS) land subsidence is a gradual settling or sudden sinking of the Earth's surface due to subsurface movement of earth materials. Subsidence is a global problem, and in the United States more than 17,000 square miles in 45 states have been directly affected by subsidence (Galloway et al. 1999). The principal causes are aquifer system compaction, drainage of organic soils, underground mining, hydrocompaction, natural compaction, sinkholes, and thawing permafrost. More than 80% of the identified subsidence in the US is a consequence of human extraction of underground water, and the increasing development of land and water resources threatens to intensify existing land-subsidence problems as well as initiate new ones. According Poland (1984, 12) problems caused by subsidence include:

> (1) differential changes in elevation and gradient of stream channels, drains, and water transport structures, (2) failure of water-well casings due to compressive stresses generated by compaction of aquifer systems, (3) tidal encroachment in lowland coastal areas, and (4) in areas of intensive subsidence, development of tensional or compressional strain in engineering structures.

In coastal communities land subsidence can increase the risk in flooding, alter wetland and coastal ecosystems, and damage infrastructure and historical sites (Eggleston and Pope 2013).

The area of focus for this study is the Southern Chesapeake Bay Region of Virginia. This region includes Southampton County, the City of Franklin, Isle of Wight County, the City of Suffolk, the City of Chesapeake, the City of Portsmouth, the City of Norfolk, and the City of Virginia Beach. Figure 2 shows the study region highlighted. According to the United States Census the population in this area in 2014 was 1,175,181 (US Census Bureau). The United States Geological Survey collected data on groundwater use in this area and in 2010 41.02 million gallons of groundwater were extracted each day (Maupin et. al. 2014).[1] This region is analyzed because it has seen the highest rates of land subsidence on the east coast of the United States (Eggleston and Pope 2013). This is in large part due to the physical characteristics of the region,

[1] As a state, Virginia ranks 21st in the nation in total groundwater extractions as of 2010 (Maupin et al. 2014).

which influence the degree to which groundwater pumping results in land subsidence. This region relies heavily on the Potomac Aquifer, which supplies roughly 75% of the region's groundwater, and is overlain by a thick layer of clay and silt (Masterson et al. 2015). Land subsidence in the region is driven by water level decline (resulting from groundwater pumping) as well as two physical factors that vary substantially across the region. These factors are sediment compressibility and sediment thickness (Galloway et al. 1999). In our mathematical simulation, we account for spatial heterogeneity in these factors in estimating land subsidence and the economic damages associated with groundwater pumping.

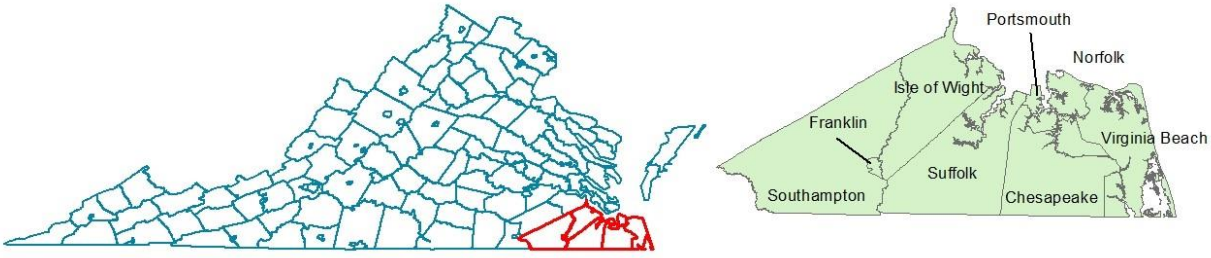

Figure 1: Study Region: Location within Virginia (left) and Names of Municipalities (right)

In the Southern Chesapeake Bay Region of Virginia, land subsidence has been observed since the 1940s at rates of 1.1 to 4.8 millimeters per year (mm/yr) (Eggleston and Pope 2013). These high rates of subsidence are due to the extensive pumping of the Potomac Aquifer as well as the formation of the aquifer system (Eggleston and Pope 2013). This area has a low-lying topography and any change in relative sea-level rise can increase the potential for flooding in urban and undeveloped areas. According to the Environmental Protection Agency (EPA) relative sea-level rise is sea height changes plus land height changes. Land subsidence is directly linked to an increase of relative sea-level rise by causing a decrease in land elevation. This large amount of land subsidence helps explain why this area has seen some of the highest levels of relative sea-level rise on the Atlantic Coast of the United States (Eggleston and Pope 2013). Analysis by McFarlane (2012) found that between 59,000 and 176,000 people could be displaced in the Chesapeake Bay region by year 2100 due to increased flooding. Residents in inland areas of the region are already dealing with the effects of land subsidence. The Blackwater River Basin is subject to flooding and areas such as the city of Franklin and the counties of Isle of Wight and

Southampton have experienced large floods in recent years. Land subsidence may be influencing this increase by altering topography and as a result, the flow of the river (Eggleston and Pope 2013).

The Chesapeake Bay itself is the largest estuary in the world and is home to hundreds of plant and animal species, including more than a dozen wildlife refuges that protect important estuaries (Chesapeake Bay Program 2011). Any small increase in relative sea-level rise could lead to a change in the tidal dynamics that these species rely on for their existence (Eggleston and Pope 2013). Also, when land subsides in coastal areas it subjects shorelines to increased wave action that leads to higher erosion and washover during storms (Eggleston and Pope 2013).

Another issue that is prevalent in coastal communities that rely heavily on groundwater resources is the risk for saltwater intrusion, an issue that has resulted in declining groundwater quality and economic damages in coastal regions worldwide (Knapp and Baerenklau 2006). According to the USGS, groundwater depletion, which occurs when water is extracted faster than it is recharged, in aquifers that boarder bodies of saltwater can lead to saltwater intrusion. The potential for saltwater intrusion in the Southern Chesapeake Bay region has increased due to increased pumping between 1900 and 1980. If saltwater intrusion occurs, the area may be forced to invest in procedures that desalinate groundwater in order to meet the demands of coastal communities (Masterson et al. 2015).

The economic literature has examined at length two important externalities associated with pumping groundwater (see Koundouri 2004 for a review of this literature). The first is a pumping cost externality; the second is a stock externality. A pumping cost externality arises when groundwater pumping by one individual reduces the amount of water in an aquifer, driving a decline in the elevation of the groundwater table (the uppermost limit of the aquifer). A fall in the groundwater table increases the marginal cost of pumping groundwater for all groundwater pumpers using the same aquifer. As a result, firms have an incentive to withdraw water too quickly because reducing their rate of pumping will lower the future pumping costs of all firms, and the firm will not be compensated for its conservation. The stock externality arises because the pumping decisions of each firm using the groundwater resource are constrained by the total groundwater stock. The “rule of capture” governs the allocation of groundwater stock: a firm can only lay claim to a unit of groundwater by pumping it (Provencher and Burt 1993).

A large economic literature examines these externalities and other externalities associated with groundwater pumping, such as stream depletion (Kuwayama and Brozovic 2013). However, no studies that I am aware of have examined the economic effects of groundwater pumping on the risk of flooding in coastal communities. This paper's contribution is in examining how groundwater pumping creates external costs in coastal communities by increasing the risk of flooding by causing land subsidence. As flooding risk increases, the expected damages from more frequent and severe flooding are capitalized into housing values. I project land subsidence rates due to groundwater pumping and use the one-time decrease in property values due to a change in flood zones to estimate the magnitude of the land subsidence externality.

1.1. In this Study

In this study, I will investigate the effect that groundwater induced land subsidence has on coastal communities of southeastern Virginia. The next two sections look at how land subsidence can be mitigated, and at the groundwater economic literature. The data used in the mathematical simulation is presented in chapter 2. Chapter 3 introduces the spatially heterogeneous mathematical simulation that estimates the damages from future land subsidence throughout the region, as well as the pumping cost externality which is occurring due to lowering of the aquifer head height. The damage estimates from the simulation are then used to evaluate two different policy options to limit land subsidence. Finally, chapter 5 includes further conclusions and limitations to the present study.

From this mathematical simulation I show that when land subsidence is present, spatially heterogeneous policies can result in social welfare gains. This contrasts with the results found by Kuwayama and Brozovic (2013) with respect to a stream depletion externality in the High Plains Aquifer. In their study region, they find little gain from spatially differentiating groundwater pumping restrictions due to the spatial arrangement of factors that affect the costs of pumping reductions. In contrast, I show that for the land subsidence externality in southeastern coastal Virginia, it is possible to significantly lower social costs by introducing spatially explicit policies. The results from this project will provide policy makers new information regarding the full cost of groundwater pumping, and contribute to the economic literature by providing an example of a case in which spatially explicit policies are necessary to maximize the net social benefits from groundwater extraction.

1.2. Approaches to Mitigate Land Subsidence

Poland (1984) presents three ways that land subsidence can be mitigated. These include a reduction in pumping, artificial recharge of aquifers, and repressuring of aquifers through wells. The most common options for coastal plain areas are to utilize additional aquifers located further from the coast, invest in watershed conservation in order to allow natural flows of water to recharge the aquifer, and implement wastewater recycling (Roumasset and Wada 2010).

1.2.1. Reduction of Pumping

Poland (1984, 127) describes eight options to limit the amount of water pumped from a single source. These options are:

1) Import of substitute water
2) Conservation in application of water use
    a. Through improvement of irrigation methods
    b. Through change of crop type
3) For overdrawn ground-water basins, introduce equitable distribution of available supply
4) In urban areas, by recirculation and reuse of treated wastewater
5) By decreasing irrigated area or industrial plants using large quantities of water
6) By moving wells to tap more permeable and less compressible deposits
7) By changing the depth range of perforated intervals in well casings to tap less compressible deposits
8) By legal control

While the import of substitute water may not, in reality, stop land subsidence (if water is drawn from alternative groundwater resources), it is an option in many coastal areas because it decreases the risk of subsidence in areas that are most susceptible to flood damage. Poland (1984) presents two ways to conserve water use: improvement of irrigation methods and changing crop type. However, the economic literature has established that improving irrigation efficiency often fails to conserve water, as irrigators respond to improved efficiency by expanding their irrigated area or producing more water-intensive crops (Cobourn; Pfeiffer and Lin 2014). Roumasset and Wada (2010) present other options for conservation, such as investing in watershed capital to enhance the natural recharge capacity of the aquifer. These investments include fencing for feral animals, removal of invasive plants, reforestation of native flora, or construction of engineering structures designed to increase infiltration. Also, for users who do not require the use of potable water (industrial users, some agriculture users) lower quality water can be substituted for extracted groundwater. For these areas, wastewater recycling may be an

alternative to groundwater use. Recycling wastewater is a substitute to groundwater, especially in areas where residential consumption meets or exceeds withdrawals for non-potable water users. However, wastewater recycling can be expensive to implement due to the fact that non-potable water requires its own infrastructure to ensure that potable water remains uncontaminated. In order for any of these options to be justifiable economically, their costs of implementation must be compared to the economic costs arising from land subsidence and other groundwater pumping externalities.

1.2.2. Artificial Recharge

Artificial recharge is achieved by putting surface water in basins, furrows, ditches, or other facilities where it infiltrates into the soil and moves downward to recharge aquifers (Bouwer 2002). Artificial recharge has been used at an increasing rate over the past few decades in order to counteract the effect of groundwater extraction. Since most subsidence is caused from the compaction of compressible confined layers within an aquifer, by ensuring that aquifers remain at a constant level (inflows equal outflows) artificial recharge could slow or even stop subsidence. However, because these confined layers may inhibit vertical downward movement of water from the land surface, it may not be feasible or effective to increase the amount of surface water over the area of subsidence. In some locations with certain geological features, confined aquifer systems may crop out near the margins of the groundwater basin; this outcrop area may be near enough to the subsiding area so that artificial recharge on the outcrop area will raise the local water table. In areas with confined layers, water can be directly injected through wells. Artificial recharge has been shown to reduce seawater intrusion as well as reduce land subsidence, and improve the quality of the water through soil-aquifer treatment (Bouwer 2002).

1.2.3. Repressuring of Aquifers

Artificial recharge can also be used to repressure aquifer layers directly through wells. As water is extracted from aquifers, the pressure gradient decreases underground. The pressure change is reflected in the lowering of water levels in wells. As the water level decreases, the aquifer system compacts, causing the land surface to subside. The amount of aquifer compaction is determined by water-level decline, sediment compressibility, and sediment thickness. In the Virginia Coastal Plain, most of the compaction occurs in the confining layers; compaction in these layers is mostly non-recoverable, meaning that even if water levels return to previous heights, the surface

level will not (Eggleston and Pope 2013). Repressuring of aquifers is one way to limit the amount that pressure drops within an aquifer due to withdrawal. Treated freshwater is injected into a confining layer in order to create a hydraulic barrier, which limits land subsidence and protects coastal areas from saltwater intrusion. This approach proves very costly but has been effective in slowing or even stopping land subsidence in certain areas (Poland 1984).

1.3. Groundwater Pumping Externalities

About 89% of freshwater on Earth is located within groundwater reserves, which makes groundwater one of the most important natural resources with respect to human wellbeing (Koundouri 2004). Most economic literature has focused on confined aquifers. Due to the physical makeup of these aquifers it can take thousands of years for water to pass through the hydrological cycle. Because of this groundwater can, in many cases, be treated as a depletable resource.

In the groundwater economic literature, many studies have considered two key externalities that arise from pumping. These are the stock externality and the pumping cost externality (Provencher and Burt 1993). Both of these externalities exist because aquifers are common pool resources, though they are not open access as pointed out in the seminal work of Gisser (1983). Groundwater access is restricted to those individuals who own land overlying the aquifer, but within that group one farmer cannot restrict the access of his neighbors to the aquifer (Gisser and Sanchez 1980). Because a single aquifer is utilized by many farmers, if an individual farmer pumps less this year he cannot expect to have more water in storage for him next year.

The stock externality arises because pumping by one firm reduces the stock of groundwater from which all other firms can pump (Provencher and Burt 1993). The only way that a producer can lay claim to a unit of groundwater is by pumping it (Provencher and Burt 1993). This leads to lesser availability of groundwater in the future (Katic and Grafton 2012). The pumping cost externality exists because the cost of pumping depends on the stock of groundwater (Provencher and Burt 1993). This means more electricity and deeper wells are needed in order to continue pumping as head height declines (Katic and Grafton 2012).[2] Both of these effects vary spatially depending on where pumping occurs, how much pumping occurs, and when pumping occurs, as well as the natural formation of the aquifer system. This leads to the

[2] Head height is the water elevation in a well (Deming 2002).

need for some regulation as groundwater resources are not as exclusive as other resources such as timber. Gisser and Sanchez (1980, 638) put it in these words: “If each farmer owned his own little aquifer, there would be no problem of externality, and his effort over time would maximize the present value of all future income streams derived from irrigation.” Instead of pumping at rates that maximize present value, farmers using a common aquifer pump at the competitive rate that equates the marginal cost of pumping and the value of the marginal physical product of water. Because this fails to reflect the value of leaving a unit of groundwater in the aquifer (both in terms of augmenting the stock and reducing marginal pumping costs), farmers will pump a larger quantity of water from a common pool aquifer than is socially optimal.

In 1980, Gisser and Sanchez published their seminal article that considers the social costs of unrestricted groundwater pumping, which arise due to the stock and pumping cost externalities. Their paper compares the temporal allocation from an optimal control management practice to the outcomes from competitive pumping. Under certain assumptions, the authors show that the difference between these two situations is so small that it can be ignored from a practical standpoint.

Gisser and Sanchez (1980) begin their analysis by calculating the competitive pumping schedule over time at which farmers equate the value of the marginal physical product of water with the marginal cost of pumping. They then calculate the pumping path over time under optimal control that would maximize the present value of future income streams. This is the pumping path that would prevail if a single farmer had exclusive access to the entire aquifer. By comparing these results, they show that when the storage of an aquifer is relatively large, these two outcomes would be identical for all practical purposes. This result, that there is little or no difference between pumping outcomes under regulated or competitive markets, implies that the welfare loss from inter-temporal misallocation of pumping is negligible, especially if the time and cost of implementing groundwater pumping restrictions is considered.

While this study has been instrumental in groundwater economics, the assumptions imposed on the model to achieve these results are highly limiting. The main driver of the result shown by Gisser and Sanchez (1980) is the assumption of a single-cell or bath-tub shape of the aquifer system. In the Gisser-Sanchez model the aquifer is modeled as an unconfined aquifer, with infinite hydraulic conductivity. This underlying assumption states that the aquifer responds

instantly and uniformly to groundwater extraction. The spatial distribution of resource users is ignored as well as temporal differences from groundwater withdrawal. Other assumptions are: recharge is constant, constant return flow and average rainfall, independence of surface water and groundwater systems, and a bottomless aquifer.

Following publication of the Gisser-Sanchez results, a number of studies perform sensitivity analysis on these assumptions. Analytical investigations of the robustness of the Gisser-Sanchez model in many cases show differing results (Koundouri 2004). For example, the benefits from optimal control vary substantially depending on the characteristics of the aquifer system, such as size, recharge rates, and number of pumpers. In the Yolo basin in California introducing regulations on pumping the value of groundwater increased by 10% (Lee et al. 1981). In the Ogallala basin the benefit was only 0.3%, and in Kern County, California the increased value from regulation did not exceed 10% (Feinerman and Knapp 1983).

More recently studies have begun to look at whether the Gisser-Sanchez results persist under different modeling assumptions. For example, Provencher and Burt (2012), Tsur (1990), and Tsur and Graham-Tomasi (1991), and Katic and Grafton (2012) consider the case in which surface water availability is stochastic, which gives rise to an additional groundwater pumping externality. Specifically, a risk externality arises because the income of all farmers utilizing a common aquifer is affected by the total stock of groundwater available. If an aquifer is completely depleted the income for all firms is relatively variable, due to the variability associated with natural recharge and surface water deliveries (Provencher and Burt 2012). As the amount of groundwater that is available for future use increases, the income risk for all firms decreases by buffering against drought. In unregulated markets a firm only considers the private benefit of risk reduction and thus fails to extract at the socially optimal rate.

Other studies have altered assumptions in the Gisser-Sanchez model about the spatial aspects of the aquifer's dynamics. By changing the underlying behavior of each aquifer, the welfare gains from optimal management may be under- or over-estimated if a bath-tub representation is used (Katic and Grafton 2012). Because spatial differences cannot be assessed using the Gisser-Sanchez model, even if the bath-tub *shape* of an aquifer accurately describes the aquifer's dynamics, the Gisser-Sanchez model will not provide accurate results for policy makers

because it fails to capture the way in which groundwater moves laterally over time (Katic and Grafton 2012).

Economist have recognized the limitations of the bath-tub models, and have since began to create more realistic simulations. Spatial models have been used to examine optimal groundwater use paths. These models include a theoretical model for the optimal extraction of groundwater by spatially distributed users (Brozovic et al. 2006), as well as a discrete kernel-based hydrologic model to compare socially optimal and competitive extraction schemes from a hypothetical basin (Faisal et al. 1997). By examining externalities as a spatial-dynamic process the number of choice variables in the optimization increases. Katic (2011) presents a model in which groundwater extraction site location is endogenous. This model was used with varying assumptions regarding spatial distribution of the aquifer and it was found that the bath-tub model significantly underestimates the welfare and hydrological costs from unregulated well location based on the maximization of own profit (Katic 2011). Because of this, a regulation that locates new wells in areas with low hydraulic interference may result in significant welfare gains even if extraction rates are unregulated (Katic 2011).

1.4. Hedonic Pricing, Flood Risk, and Flood Zone Designation

Although a number of externalities associated with groundwater pumping have been considered in the economic literature, I am aware of no studies that have examined the land subsidence externality. The land subsidence externality arises as groundwater pumping in one location causes drawdown and subsidence in another location, which leads to an increase in flood risk and increase in likelihood of flood zone designation.

Even though not considered in the groundwater literatures there is a hedonic literature to draw on, which estimates the damage associated with flood zone designation. This section presents an overview of the hedonic pricing literature to establish the basis for estimating the economic cost of land subsidence. This literature provides a range of estimates for the change in property value from a change in flood zone designation. I include as part of this discussion a section on insurance premiums and flood risk.

Hedonic pricing models gained traction with Rosen's seminal paper (1974). Rosen hypothesized that a product could be differentiated into a vector of objectively measured characteristics. By breaking homes into different structural and environmental attributes,

economists are able to estimate consumers' willingness to pay for varying degrees of environmental goods and services. Since this paper's publication, hedonic pricing has become a tool often used to value nonmarket goods. There have been numerous hedonic property studies on environmental risks, including earthquake and volcano hazards (Beron et al. 1997), flood hazards (Bin and Polasky 2004) hurricane hazards (Hallstrom and Smith 2005), hazardous waste (McClusky and Rausser 2001), and erosion hazards (Landry et al. 2003).

Three main papers in this literature value the property damage arising from spatial variation in flood risk. Bin, Kruse, and Landry (2008) use hedonic property pricing methods to examine the effects of flood hazards on coastal property values. Bartosova et al. (2000) use geographic information systems (GIS) to calculate accurate measures of flood risk as well all consistent measures for locational features in neighborhoods. Lastly, Bin and Polasky (2004) use a hurricane to create a natural experiment to see if people are more willing to avoid flood prone areas after a recent major flood event.

In coastal regions when trying to estimate environmental risks, such as flood, erosion, and wind hazards, it is difficult to separate out environmental amenities that are highly correlated, such as proximity to water, water-frontage, and view (Bin et al. 2008). Bin et al. (2008) address this challenge in estimation by using a spatial autoregressive model that controls for amenities associated with proximity to water. Their dataset is from Carteret County, North Carolina, which is located on the Atlantic Ocean in eastern North Carolina and is a low-lying, hurricane-prone coastal zone. The maximum elevation in the county is 51 feet above sea-level with a large portion of the region's 59,383 residents living in low-lying areas prone to flooding. Over 3000 home sales from 2000-2004 were collected. GIS data are used to assign values to each observations for characteristics such as distance to water, nearest central business district, nearest highway, and nearest park, forest, or game land. By including these spatial characteristics the authors are able to separate the positive utility that is gained by living close to water from the negative disamenity that is created due to increased flood risk.

To characterize flood risk, they use National Flood Insurance Program (NFIP) flood zones as a proxy for flood risk as well as coastal water frontage and distance to sound and intracoastal waterways as amenity measures. The NFIP flood zones are useful because they are divided into 100-year flood zones (a 1% chance of flooding per year) and 500-year flood zones

(a 0.2% chance of flooding per year), which provides the opportunity to estimate differences in willingness to pay at different levels of risk. The authors find that when coastal amenities are not controlled for, there are no measurable effects from either flood classification (100-year or 500-year). However, once amenities have been included, they find that being located within a floodplain lowers property values by 7.3% on average. They then break down flood risk into observations located within 100-year flood zones and 500-year flood zones. They find that being in 100-year flood zones reduces property values by 7.8% on average, while being in a 500-year flood zones reduces property values by 6.2% on average.[3]

Bartosova et al. (2000, 1) state: "one of the consequences of continued urbanization is the tendency for floodplains to expand, increasing flood risks in the areas around urban streams and rivers." They recognize that hedonic pricing can be used to model the relationship between house prices and flood risk, but it has a weakness in that it has incomplete controls for locational characteristics that influence house prices. They address this issue by using GIS tools to provide more accurate measures of flood risks and more accurate accounting of neighborhood features. By including more information on each observation in the data set, the hedonic model can produce unbiased, consistent estimators. These estimated coefficients can provide policy makers the consumer's true willingness to pay to avoid flood risks which can lead to community-wide benefit measures from flood control projects (Bartosova et al. 2000).

The study area in which Bartosova et al. (2000) work is approximately 11.5 miles along the middle lower sections of the Menomonee River through Wauwatosa and Milwaukee, Wisconsin. These two areas are chosen in order to encompass two differing areas. Wauwatosa is a high density residential area while the neighborhood chosen in Milwaukee is small and isolated when compared to other areas in the region. Both of these areas are located along the Menomonee River and reside within Federal Emergency Management Agency (FEMA) National Flood Insurance Program areas.

The authors use GIS to spatially define flood risks, assign street addresses for each observation, and to create location specific data. By including location specific data such as

[3] They also find that residents are aware of flooding risk. The study region of Bin et al. (2008) requires disclosure of flood risk for any home sales. Disclosure of flood risk is important because research conducted by Chivers and Flores (2002) found that the majority of households living in flood prone areas of Colorado were unaware of the risk when submitting bids for properties and thus no negative effects of flood risks were observed.

school districts and distance to parks, the authors are able to counteract the potential colinearity associated with amenities gained by being located close to water and disamenities such as increased flood risks. Housing attributes are obtained from the Multiple Listing Service (MLS) for the Milwaukee Metro Area between January 1995 and July 1998 (Bartosova et al. 2000). There was a major flood event in the region in June of 1997 and the authors select the dates of their observations in order to calculate any effects caused by this event. Overall there are 1,431 usable observations. The authors organize the variables into six categories: structural, neighborhood, fiscal, disequilibrium, time related, and flood. The flood variables are the main interest of this study and this category includes a continuous measure of risk derived using GIS. Specifically, the authors examine the effect of being within floodplains in 100 year increments ranging from 100-year to 500-year periods. They also estimate the short run effects of a specific flood event by including a dummy variable for whether the property sold before or after the flood of 1997 and an interaction between this variable and the floodplain variable. This interaction can be used to test whether people are more aware of flood risks after a major flood event.

The authors find that the marginal effect of a reduction in flood risk (i.e. moving from a 10-year risk to an 11-year risk) increases the value of a home by 2.3%. In an area where the risk is 33.3-years, this flood risk reduction premium diminishes to zero (Bartosova et al. 2000). A major result that was found was with respect to homes sold before and after the flood of 1997. Homes located on the edge of the river that sold before the flood are on average worth 5.1% less than comparable homes located outside of the 100-year floodplain. However after the flood, homes on the edge of the river sold for 18.9% less than comparable homes outside of the floodplain. Finally, the authors calculate the effects of moving from a 100-year floodplain to a 200-year floodplain and so on. Since the authors' first model showed that the effects of flood risk dissipated within the 100-year floodplain, it is not surprising that only the 100-year floodplain coefficient is significant. The results of this study suggest that, even at their largest, the intensive margin effect of a change in flood risk is small compared to the extensive margin effect.

Bin and Polasky (2004) build on the idea that consumers have a higher willingness to pay to avoid flood risks after a major flood event. They use the occurrence of Hurricane Floyd to estimate the marginal WTP to avoid floodplains before and after the storm in Pitt County, North Carolina. Hurricane Floyd hit eastern North Carolina in September 1999 and caused record

amounts of flooding. Total damages are estimated at $6 billion, most of which were caused by flooding. This region has a low-lying topography and is relatively flat which leads to increased risks of flooding. The authors point out that prior estimates of these effects may have included the sale of properties that still contained flood damages.

The study region in which data is collected is Pitt County, North Carolina. The Tar River flows through the middle of the county and runs into the Pamlico Sound. The highest elevation in the county is 126 feet above sea level. Floodplains in the county include areas along the Tar River and its tributaries. The data set contains the sale of 8,375 single-family homes between July 1992 and June 2002 with about 6% of the homes being located within a floodplain. The authors use ordinary least squares regression with a semi-log functional form to estimate the coefficients.

Bin and Polasky (2004) find that when Hurricane Floyd is omitted from the model, the effect of being located within a 100-year floodplain reduces the average value of a home by 5.7%. After accounting for Hurricane Floyd, the difference in the estimated discount between pre-Floyd and post-Floyd sales is statistically significant. The estimated difference in similar homes before Floyd is 3.7% while after Floyd the difference increases to 8.3%. This result supports the authors' hypothesis that major flood events could change the perception of flood risks by property owners and the discount for properties within floodplains. These results are relevant to this study because the difference between pre-flood event and post-flood discounts can be examined when comparing potential policy options that attempt to lower land subsidence due to groundwater pumping. If a government agency is attempting to issue new policies that limit the increase in flood risk after a major flood event; it may be easier to justify the cost due to a higher willingness to pay for avoiding flood-prone areas.

Overall, these three studies provide reliable estimates of the decrease in property value premium caused by an increase in flood risk. All studies calculate the loss of value of a home from being located within a flood zone, with an average loss between 3.7% and 8.3% (dropping the post-flood event loss of 18.9% calculated by Bartosova et al. 2004). Overall, these values range from 2.3% to 11.3%. This provides a range of values that can be used to estimate the property value losses arising due to groundwater pumping induced land subsidence in coastal, southeastern Virginia.

CHAPTER 2. SPATIAL INTERPOLATION OF AQUIFER CHARACTERISTICS AND CENSUS DATA

In order to create a mathematical model, I first start by creating the dataset that is imported into the model. I begin by gathering data on the aquifer system. To do this I rely on data collected by McFarland and Bruce (2006). They present data on 403 borehole locations and include top-surface elevation of the aquifer units in the Coastal Plain of Virginia. Elevations are collected for the land surface, Yorktown Confining Zone, Yorktown-Eastover Aquifer, Saint Mary's Confining Unit, Saint Mary's Aquifer, Calvert Confining Unit, Piney Point Aquifer, Chickahominy Confining Unit, Exmore Matrix Confining Unit, Exmore Clast Confining Unit, Nanjemoy-Marlboro Confining Unit, Aquia Aquifer, Peedee Confining Unit, Peedee Aquifer, Virginia Beach Confining Zone, Virginia Beach Aquifer, Upper Cenomanian Confining Unit, Potomac Confining Zone, Potomac Aquifer, and basement bedrock. These data are collected and recorded for each borehole number and the coordinates (latitude and longitude) are provided for each borehole. I use data on the land surface, the Potomac Confining Zone, the Potomac Aquifer, and the basement bedrock. In order to estimate the thickness of the Potomac Confining Zone, the thickness of the Potomac Aquifer, and the elevation of the basement bedrock. Overall there are 142 boreholes in the study region used for these estimations. In this original set of 142 points, there are only 13 points that include information on the elevation of the bedrock. In order to acquire more reliable results, I expand my search to include boreholes that lie outside of the study region. An additional 29 points are used for the bedrock interpolation, for a total of 42 observations in the broader geographic region. Figure 2 shows the locations of the boreholes. With these data points I am able to estimate a continuous surface for the top of the Potomac

Confining Unit, the top of the Potomac Aquifer, and the top of the basement bedrock. To do this I am using the spatial interpolation tools in ArcGIS.

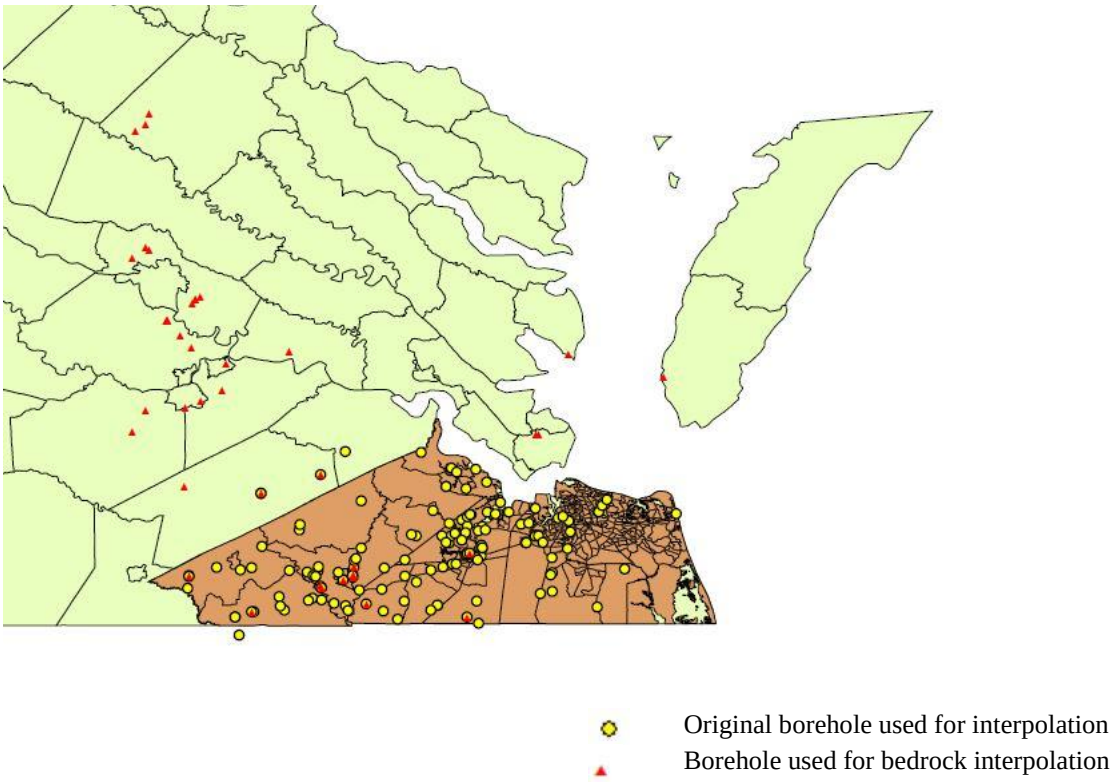

Figure 2: Location of Borehole Data Points Collected by McFarland and Bruce 2006

2.1. Spatial Interpolation Methods

Spatial interpolation can be used to create continuous surfaces from sampled point data. Examples of sampled point data include forest inventory plot data, wildlife observations, groundwater depth measurements, air quality standards, or soil sample analysis. The continuous surface created through interpolation can represent some measure such as height, concentration, or magnitude. The surface created provides estimated values throughout the region whether or not sampled measurements have been collected. Lant et al. (2005) use GIS in order to optimize farm level land use with respect to soil erosion and the Conservation Reserve Program. Kumar et al. (2016) use ArcGIS to compare interpolation techniques while modeling air quality throughout Mumbai City, India. With this information they began to estimate the economic health cost that higher levels of air pollution can cause. GIS has also been used heavily in the hedonic pricing

literature to estimate the effects of environmental factors that vary spatially. Bartosova et al. (2000) use GIS to evaluate the effects of flood risk on residential property values and provide an accurate measure of consumers' willingness to pay for a reduction in flood risk.

The software ArcGIS provides multiple ways to derive a prediction for each location. These methods can be classified into two main groups: deterministic methods and geostatistical methods. Geostatistical methods are based on statistical models that include autocorrelation. Because of this, geostatistical techniques not only have the capability of producing a prediction surface but also some measure of the certainty or accuracy of the predictions. An example of geostatistical interpolation is kriging. Geostatistical methods are designed to work with datasets that measure the density of a specific characteristic in a region (trees per acre, air pollutants in a region, or population data). Because I am interested in predicting unique values at each point in the study region, I focus on deterministic interpolation methods, which assign values to locations based on surrounding measured values and on specified mathematical formulas that determine the smoothness of the resulting surface. Inverse distance weighted (IDW), natural neighbor, trend, and spline are all examples of deterministic interpolation methods.

IDW interpolation predicts cell values using a linearly weighted combination of sampled points. The weight of the function is determined by the inverse of the distance from the sampled point to the predicted point. By using the inverse of the distance from sample to predicted point it is assumed that the influence of the sample decreases as distance increases. IDW lets users determine how much influence distance has on the predicted values by allowing the power parameter to be changed. The default value for the power value is 2; increasing this value places more emphasis on closer observations, which yields a more detailed and heterogeneous surface. If this value is smaller than 2 then the output layer will be smoother across space.

Because IDW is not linked to a physical process there is little guidance for choosing the correct power value. ArcGIS includes a Geostatistical Analyst function which can be used to determine the minimum mean of absolute errors which can provide some estimate of fit for the predicted layer. When using IDW interpolation, users can also control the number of measured points that are included when calculating the predicted cell value. By using a variable search radius, users can control the number of measured points, which must be included when calculating the new values. Once the desired number of points are chosen, ArcGIS finds the

closest measured points to each predicted cell and assumes that those are the only points that affect the estimated value. If a fixed search radius is selected, ArcGIS uses all measured points within a given radius of each predicted cell. Users must also choose a minimum number of points that will be included in each predicted value. If the minimum number of observations are not located within the fixed radius, the model will expand the radius until the minimum number is met.

Natural neighbor interpolation uses Voronoi diagrams to partition the study region into subsets based on distance to measured points.[4] Once the Voronoi diagram has been created, ArcGIS finds the closest subset of input samples to a predicted point and applies weights to them based on proportionate areas to interpolate a value. Natural neighbor interpolation provides localized estimates and will only calculate estimated values within the range of measured values. This means that natural neighbor interpolation will not create peaks, pits, ridges, or valleys that are not already represented by the input values.

Trend interpolation methods use polynomial regression models to fit a least-squares surface to the input points or logistic regression for generating a surface for predicting the presence or absence of a phenomena. The most basic from of trend interpolation fixes a flat plane across measured values. However a flat plane cannot include the variability that is seen in most measured attributes, so the trend function allows users to specify a number of bends in the formula in order to better predict unknown cells. This is done by changing the regression function from a first-order polynomial into a multinomial function.[5] Trend interpolation chooses the best surface in order to minimize the difference between the sampled and predicted values, or the root mean square error (RMSE). The lower the RMSE, the closer the estimated layer is to the observed layer.

2.2 Aquifer System Data

For this study, I rely on the inverse distance weighting (IDW) method to describe aquifer characteristics throughout the study region based on sample points. As mentioned previously, the

[4] A Voronoi Diagram, sometimes referred to as a Dirichlet tessellation, partitions "a plane with *n* points into convex polygons such that each polygon contains exactly one generating point and every point in a given polygon is closer to its generating point than to any other" (Wolfram 2016).

[5] ArcGIS allows users to add up to 12 bends in trend functions

data used for the spatial interpolation is from McFarland and Bruce (2006). The interpolated layers are shown in figures 3-6.

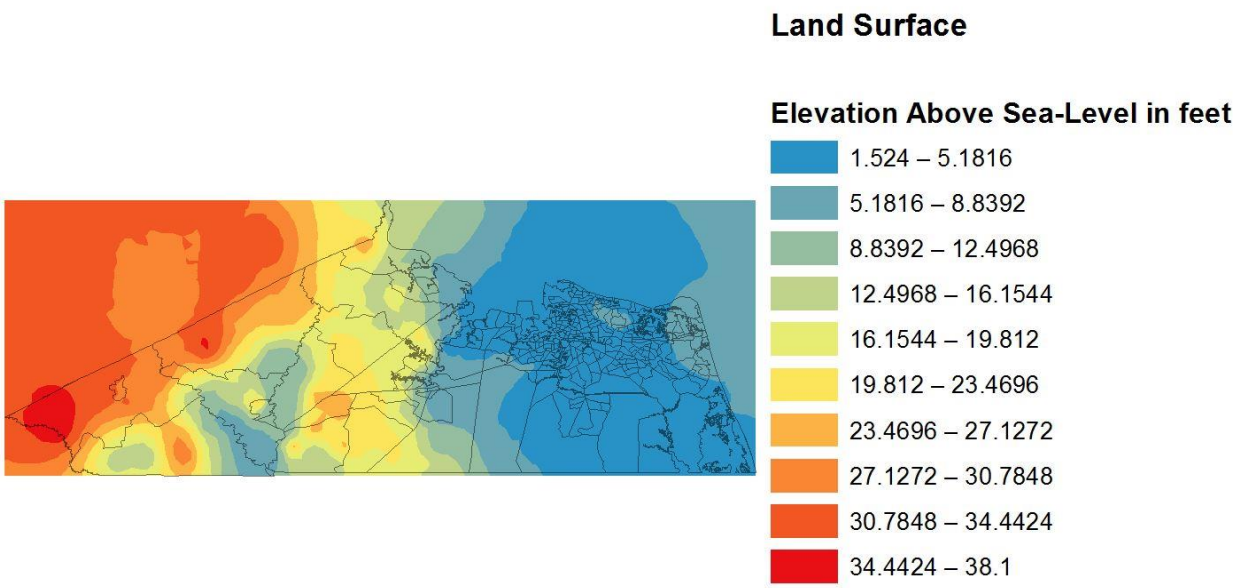

Figure 3: Interpolated Layer of the Land Surface

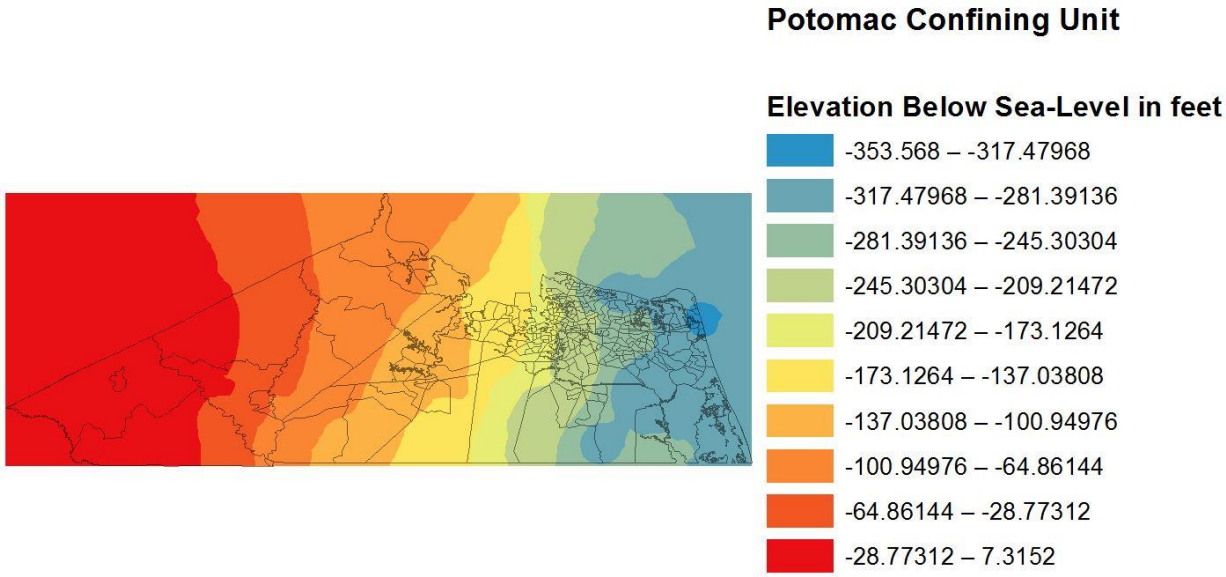

Figure 4: Interpolated Layer of the Potomac Confining Unit

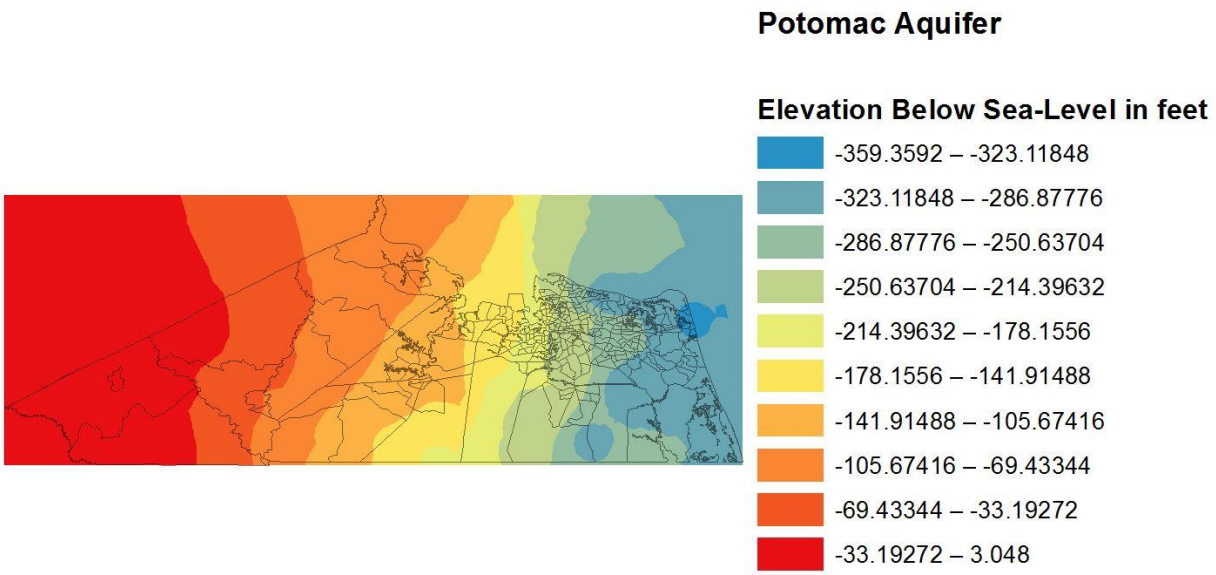

Figure 5: Interpolated Layer of the Potomac Aquifer

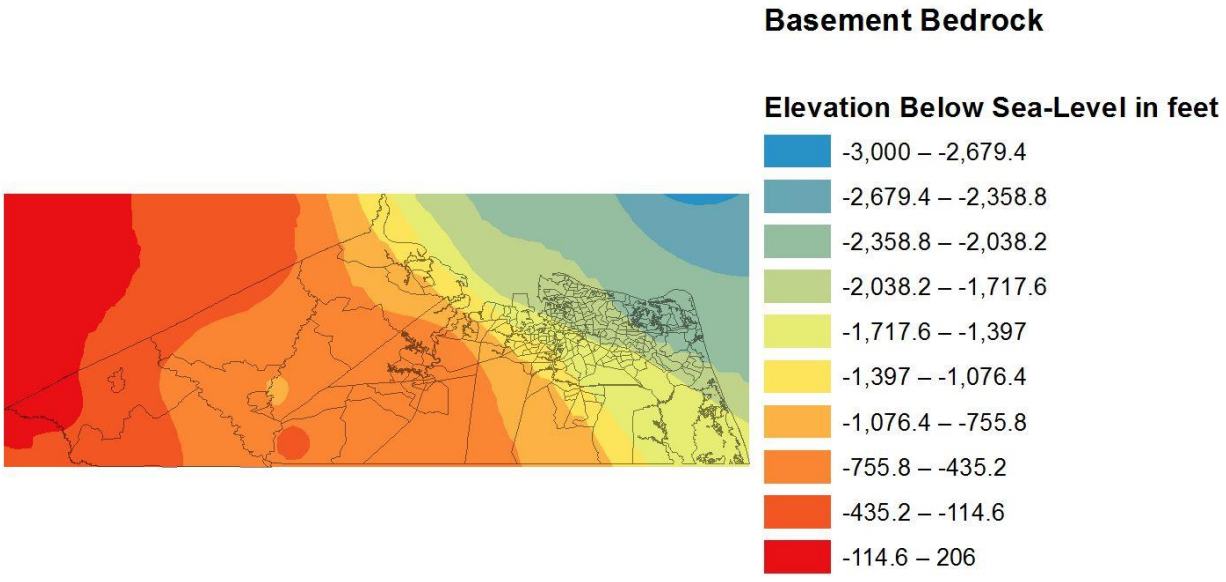

Figure 6: Interpolated Layer of the Basement Bedrock

The spatial interpolation algorithm in ArcGIS allows users to change the number of points that are used in the interpolation. In order to minimize the RMSE from the IDW interpolation, I run the calculation using four different specifications in which the number of the minimum and maximum points included varies. The four scenarios are described in table 1. In

order to estimate land subsidence, I estimate the height of pumping[6], the thickness of the aquifer confining unit, and the thickness of the aquifer itself. In order to calculate these parameters, I interpolate the elevation of the land area, the elevation of the top of the confining unit, the elevation of the top of the aquifer, and the elevation of the basement bedrock. For each of these parameters, I run the IDW estimation once for each scenario. The resulting RMSE for each scenario for each location is in table 1. For each elevation estimated, scenario 2 with a minimum of 5 points and a maximum of 10 points used in the interpolation yielded the lowest RMSE. The results from these interpolations are illustrated in appendices A-D.

Table 1: Inverse Distance Weighting Root Mean Square Error Results

Case	Minimum included points	Maximum included points	Bedrock IDW Estimate	Potomac Aquifer IDW Estimate	Potomac Confining Unit IDW Estimate	Land Surface IDW Estimate
1	10	15	76.9794	16.5002	16.2347	4.53935
2	5	10	72.3220	15.7502	15.4093	4.48876
3	15	20	83.9533	17.2258	16.9741	4.66942
4	5	20	72.4740	16.9083	16.6687	4.66920

Once the interpolations are complete, I convert the interpolated layer from a point into a raster dataset. The advantage to using raster datasets is that it is possible to perform mathematical operations using multiple layers whereas it is not possible to do so using point data layers. In order to estimate the height of pumping, I subtract the elevation of the top of the Potomac Aquifer from the elevation of the land surface. This yields the minimum pumping distance, which can be used to estimate how pumping cost will change over time due to a lowering of the aquifer head height. The thickness of the confining unit is calculated by subtracting the elevation of the top of the Potomac Aquifer from the elevation of the top of the Potomac Confining unit. Lastly, the thickness of the aquifer is calculated by subtracting the elevation of the basement bedrock from the elevation of the Potomac Aquifer.

After creating these three new layers, height of pumping, confining unit thickness, and aquifer thickness, I use the fishnet tool in ArcGIS to create a grid of 300m by 300m cells. These cells are used as the spatial unit of observation in the mathematical simulation model described

[6] The height of pumping can also be called the depth to water table.

in Chapter 3 to predict groundwater levels, land subsidence, and the pumping cost and property value externalities. In order to estimate these changes, the average surface height, average thickness of the aquifer, and the average pumping distance is calculated within each cell using zonal statistics in ArcGIS.

2.3 Census Data

In order to estimate the economic damages from land subsidence, I need information at the resolution of the model cells on population, number of homes, and home values. These data are collected by the United States Census Bureau. There are 294 census tracts located within the study region. The summary statistics for the number of housing units, average home price, and the population are in table 2.[7] These data will be used, along with results from hedonic pricing literature, to calculate the expected property damages from land subsidence.

Because the census data are reported at a coarser spatial resolution than the model grid, it is necessary to make assumptions about the spatial distribution of homes within each census tract. I assume that homes are uniformly distributed within each census tract. This assumption allows me to calculate the number of homes located within each cell by multiplying the percent area of a census tract that each cell covers by the total number of homes in the census tract. With this number I can then multiply the number of homes in each cell by the average home price to estimate the total value of homes within each 90,000 m^2 cell.

By assuming a uniform distribution of homes within each census tract, the simulation model will understate spatial heterogeneity in housing values within the study region. The effect of this assumption is to smooth spatial variation in the land subsidence externality. If the model results present evidence of significant spatial variation in the effects of land subsidence on flooding risk even while maintaining this assumption, then evidence of spatial heterogeneity in the externality is strengthened. Therefore, I proceed with the assumption of a uniform distribution in housing density and values.

Table 2: Census Data Summary Statistics

	Housing Units	Housing Price	Population
Mean	1439.82	$243,497.53	3,972.93
Median	1369.00	$219,200.00	3,756.00
Mode	1587.00	$146,900.00	3,553.00
Minimum	0.00	$61,900.00	5

[7] All census data from 2013.

Maximum	3588.00	$717,500.00	22,817.00
Total	423,307		1,160,096

CHAPTER 3. MATHEMATICAL SIMULATION MODEL

This chapter develops a dynamic mathematical simulation that will estimate the amount of land subsidence from groundwater pumping throughout the study region over a finite time horizon of variable length. To do this, the model must address three main questions. The first question concerns how varying the location of pumping affects drawdown of the aquifer. The drawdown of the aquifer is needed to address the second two questions, namely how drawdown affects land subsidence and how pumping costs will increase due to a decline in head height. To answer these questions, I create a mathematical simulation that predicts the change in groundwater height, land subsidence, and marginal pumping costs throughout the region due to a unit of groundwater pumping at one location (henceforth referred to as a "pumping site").[8] Simulated land subsidence due to groundwater pumping is then used to determine changes in property values from the increased expected loss from flooding.

The dynamic simulation model consists of four sections. The first solves for head drawdown in each year from pumping at a single site using the Theis Equation for each model cell described in Chapter 2. The simulation predicts the time path of drawdown each year over a 10-, 50-, and 100-year period as a function of groundwater pumping in all prior years and the physical characteristics of the region. In the second section, drawdown at the end of each year in is linked to subsidence using a well-known analytical formula that takes into account aquifer characteristics that vary across the study region. The output of this second section is cumulative subsidence over the time horizon of the model. In the third section, I quantify the marginal pumping cost externality as the change in pumping cost in each model cell due to the change in pumping lift over the time frame of the simulation. The fourth section of the simulation model quantifies the land subsidence externality. The subsidence externality arises as properties are reclassified into FEMA-designated 100-year flood zones. To estimate the expected damages arising from this reclassification, I use an econometric model that explains the probability of being in a flood zone as a function of physical variables, primarily land surface elevation. Expected damages due to cumulative subsidence in the terminal period due to changes in flood

[8] It is important to note that this is not an optimization program but a simulation of how these spatially heterogeneous variables change in response to a unit of pumping.

zone designation are estimated using a range of property value losses from the economic literature.

3.1. Theis Equation

Theis (1938) presents a simple analytical model that can be used to estimate the size and magnitude of a cone of depression due to groundwater pumping in a confined aquifer system. In their natural state, groundwater aquifers are in balance, such that discharge from the aquifer equals recharge to the aquifer. When groundwater is extracted, a cone of depression is formed at the well. Over time, this cone propagates radially outward from the pumping site, as groundwater moves laterally to fill in the pumping depression. Ultimately, a new equilibrium will hold once water levels over the full extent of the aquifer have fallen. The amount of time to reach this new equilibrium depends on the characteristics of the aquifer, which govern transmissivity, defined as the rate at which groundwater moves laterally. Because artesian aquifers are under pressure, the amount of time that it takes a cone of depression to expand is much shorter than that of unconfined aquifers.

Solving the Theis equation allows me to describe the decline in groundwater head height in each model cell in the region and in each year due to pumping at a single pumping site. In order to solve the Theis equation, it is necessary to specify several parameters: constant pumping rate for the pumping site ($pump$) in cubic feet per second, aquifer transmissivity ($trans$) in square feet per day, and storativity ($stor$). The pumping rate chosen is 1.547 cfs, which is equivalent to 1.00 Mgal/day and is based on the historical groundwater use rates published by the USGS (Maupin et al. 2014). In 2010, the total water withdrawals within the study region were 20.92 Mgal/day.[9] The aquifer transmissivity used is 10,000 ft^2/day and is chosen based on values reported by McFarland for the study region (2013). The storativity coefficient is 2 x 10^{-4} which is also taken from McFarland (2013).

The steps to solve the Theis equation are based on the process described by the Utah Division of Natural Resources: Division of Water Rights, *Theis Analysis of Well Drawdown Influences* spreadsheet calculator. This is a three-step calculation that first solves for $u(N, t)$

[9] Public supply of groundwater is 14.29 Mgal/day and domestic self-supplied groundwater is 6.63 Mgal/day (Maupin et al. 2014).

which is a dimensionless time parameter that varies by model cell (indexed by *N*) and time since pumping began (indexed by *t*):

$$u(N,t) = \frac{Dis(N)^2 * stor}{4 * trans * day(t)}$$

Once $u(N,t)$ is calculated it is substituted into the well function, $w(N,t)$:[10]

$$w(N,t) = -0.9793 * \ln(u(N,t)) - 0.2722$$

Lastly, $w(N,t)$ is substituted into the final equation to solve for drawdown:[11]

$$draw(N,t) = \frac{(pump * w(N,t))}{12.57 * \frac{trans}{864000}}$$

Figure 3 shows a graphical representation of drawdown from pumping at a single location (in yellow). In this example pumping occurs for a duration of 10 years. The resulting drawdown across model cells ranges from 0.4813 m to 3.7011 m, with the greatest drawdown in model cells closest to the pumping site (in darker brown). The radial expansion of the cone of depression from pumping is evident in the figure. The model also presents the drawdown within each cell at the end of each year of pumping.

[10] The well function is also known as the exponential integral outside of the hydrogeology literature.
[11] We convert drawdown from feet to meters in order to use the result to calculate land subsidence.

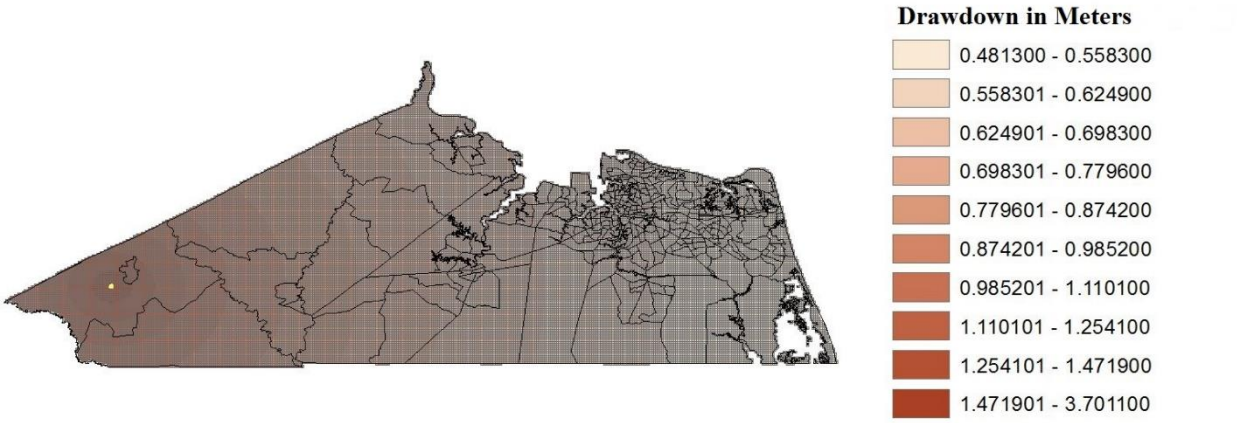

Figure 7: Example of Groundwater Drawdown from Single Pump (highlighted in yellow)

3.2. Subsidence Calculation

Using drawdown calculated with the Theis equation ($draw$), land subsidence is estimated using the following formula derived by Deming (2002):[12]

$$sub(N,t) = fd * g * draw(N,t) * cthick(N) * c$$

The subsidence equation uses the following scalars: fluid density (fd) in kg/m^3, acceleration due to gravity (g) in m/s^2, compressibility of the confining unit material (c) in m^2/N, and the original thickness of the confining unit in each cell ($cthick$) in meters. Fluid density and acceleration due to gravity are both constants with values of 1,000 kg/m^3 and 9.81 m/s^2 respectively (Deming 2002). The compressibility of the confining unit varies based on material. The overlaying confining unit of the Potomac Aquifer is made up of clay and silt and according to lab results performed by Freeze and Cherry (1979) the compressibility of this material is between 1 x 10^{-8} and 1 x 10^{-6}. The mean of this range, 1 x 10^{-7}, is used throughout the simulation. Land subsidence differs across space due to spatial heterogeneity in $cthick(N)$ as well as $draw(N,t)$. This formula implies that as a porous medium retracts, in this case the clay confining unit above the Potomac Aquifer, the land surface will subside.

[12] For full explanation of derivation of subsidence formula see pg. 240-243 *Introduction to Hydrogeology* 1st edition by David Deming.

3.3. Marginal Cost Calculator

Using projected drawdown, I calculate the increased marginal pumping cost that is caused from a lowering of head height.[13] In order to calculate the change in pumping cost due to drawdown, I rely on the basic power consumption formula presented by Goodell (1988), that relates total power consumption per year in kilowatt hours (kWh) to pumping lift (TH), volume of water pumped (Q) and kilowatt hours required to lift 1 acre-foot of water one foot (K). Contor et al. (2008) expand the formula from Goodell (1988) to reflect in greater detail the engineering parameters that affect marginal pumping costs. Specifically, their formulas reflect the marginal cost of electricity (mc_{elec}), equivalent psi (psi), and pumping plant efficiency (pp_{eff}).[14]

In order to calculate the marginal cost of pumping, first I calculate the lift height in each cell in each period:

$$lift(N,t) = pump(N,t) + draw_m - sub(N,t)$$

The power consumption necessary to pump water for the given lift in each tract and each year is calculated as:

$$pc(N,t) = \frac{psi * 2.31 + \left(\frac{21}{20} * lift(N,t)\right)}{0.3048} * \frac{1.02}{pp_{eff}} * 8.11$$

Power consumption is then multiplied by the marginal cost of electricity in order to calculate the marginal cost of groundwater pumping:

$$mc(N,t) = pc(N,t) * mc_{elec}$$

Lastly, I am interested in how pumping cost changes over time due to a decline in aquifer head height. This model simulates constant pumping over period t and calculates drawdown at the end of each period. To calculate how this drawdown will affect pumping cost in all periods after pumping has ended, I calculate the difference between the marginal cost of pumping in the final period, t_{final}, and the marginal cost of pumping in the initial period (t = 1).

$$\Delta mc(N) = mc\left(N, t_{final}\right) - mc(N, t_1)$$

[13] Subsidence actually works in favor of lowering pumping cost by lowering the pumping distance, while it is in the calculation this effect is very small in magnitude when compared to a change in head height.

[14] The marginal cost of electricity is gathered from the Federal Energy Regulatory Commission. Equivalent psi is derived from discharge pressure at the pumping station and depends on the units of measure of discharge pressure. Pumping plant efficiency is also known as wire-to-water efficiency which is a measure of how effectively a pumping plant can overcome friction between water and pipes.

This change in marginal cost is not a one-time cost to pumpers in the region but is instead the increased cost for each unit of groundwater pumped over an infinite time horizon. In order to calculate the present value of the stream of damages from an increase in pumping cost, I use the following formula:

$$PV = \frac{\Delta mc(N) * Pop(N) * Per\ capita\ water\ use}{r}$$

where r is the discount rate (3.125%).

Equivalent psi (29.964) and pumping plant efficiency (62.47%) values are taken from Alanis (2009), which evaluated eight utility companies in Virginia for metric benchmarking in order to compare efficiency across the state. Two of the eight utilities considered in the report are located within the study region. I average the values found for these two stations to obtain region-specific values for equivalent psi and pumping plant efficiency. The marginal cost of electricity is collected from the Federal Energy Regulatory Commission (FERC) Market Oversight report (FERC 2013). FERC has annual average day ahead on peak prices for regional transmission organization that coordinates the movement of wholesale electricity. Between 2008 and 2012 the average price of electricity in the region was $54.97 per Mwh. For the discount rate I use 3.125%, which is the United States Department of Agriculture's discount rate for water projects.

3.4 Property Damages from Land Subsidence

The previous section estimates the change in pumping cost due to a decline in groundwater head height, which is a widely recognized externality generated by groundwater pumping decisions (Gisser and Sanchez 1983; Provencher and Burt 1993; Koundouri 2004). A second externality generated by groundwater pumping, and the focus of this thesis, arises as land subsidence results in a one-time loss in property values. This loss in property values may arise due to an intensive margin effect (an increase in expected frequency of flooding in a flood zone) or an extensive margin effect (an increase in the size of flood zone). The former occurs when the frequency of flooding within an area currently designated as a flood zone increases due to a decline in the land surface elevation. The latter occurs as properties previously outside of designated flood zones are reclassified as inside a flood zone due to a decline in the land surface elevation. In addition to these effects, land subsidence can cause physical damage to structures due to the weakening of foundations, as well as uneven sinking of the land (Eggleston and Pope 2013).

Though all of these effects generate economic damages, this study focuses specifically on the extensive margin effect. This choice is driven in part by data availability, but is also intended to capture the majority of the economic damages arising from changing flood risk due to land subsidence. As described in this section, the economic literature on the effect of changing flood risk on property values finds evidence that the magnitude of the intensive margin effect is small relative to that of the extensive margin effect and that the intensive margin effects apply to a much smaller land area (due to diminishing marginal property premiums for reductions in flood risk). These results suggest that considering the extensive margin effect captures a large portion of the economic damages arising from land subsidence. Data exists on the changing boundaries of flood zones in the study region over time, which can be used to evaluate this extensive margin effect. In contrast, little data exists on the frequency of flooding within a flood zone. To evaluate this effect therefore requires the use of a stochastic simulation model of flood risk (e.g., Vecchia 2008). This type of activity is outside the scope of this analysis.

There are a number of variables that factor into flood zone determinations. Examples include distance to surface water, elevation, land cover, slope of the land, and soil type. In this section I test the hypothesis that elevation is the primary driver of flood zone designation. To do so, I specify and estimate an econometric model that explains whether each model cell is within a flood zone as a function of site specific characteristics. I combine data on flood zone designations from the FEMA Flood Map Service Center with site attributes derived using GIS including elevation, percent slope, distance to water, and land cover.

Whether a model cell is inside or outside of a flood zone is a binary (0/1) classification. One way to cast this problem is to view the discrete flood zone classification as emerging from a regression model for a latent variable, y^*, which captures the probability of a flood event. The model describing the probability of flooding as a function of site attributes can be written as:

$$y_i^* = \beta_0 + \beta_1 x_{1i} + \cdots + \beta_k x_{ki} + e_i$$

where i indexes model cell, the $x_{1i}, \ldots, x_{ki}$ are site specific characteristics for each model cell, and e_i is an unobservable stochastic error term. If the latent variable exceeds a threshold, an area will be categorized as within a flood zone. Below that threshold, the area will be categorized as outside a flood zone. However, the latent variable is unobservable; I only have information on

the binary flood zone classification. If cell i is within a flood zone, the observed variable y_i takes on a value of 1; otherwise $y_i = 0$.

In order to explain flood zone designation using site specific characteristics, I use a logit model. Logit models are a binary response model which give the probability of an occurrence happening given a set of explanatory variables (Wooldridge 2013). In the context of this study, the logit model captures how a change in elevation affects the probability of being located with a flood zone. Let P_i denote the probability of being within a flood zone. The logistic distribution function is written:

$$P_i = E(y = 1|x_{1i}, \dots, x_{ki}) = \frac{1}{1 + e^{-Z_i}}$$

where $Z_i = \beta_0 + \beta_1 x_{1i} + \cdots + \beta_k x_{ki} + e_i$. Given that the probability of being outside a flood zone is $1 - P_i$, the odds ratio in favor of being inside a flood zone can be written as:

$$odds = \frac{P_i}{1 - P_i} = \frac{1 + e^{Z_i}}{1 + e^{-Z_i}} = e^{Z_i}$$

Taking the natural log of this expression yields:

$$ln\left(\frac{P_i}{1 - P_i}\right) = Z_i = \beta_0 + \beta_1 x_{1i} + \cdots + \beta_k x_{ki} + e_i$$

The logit model assumes that e_i follows the logit distribution with mean zero. Using simple arithmetic, the probability of being in a flood zone can be calculated using the odds ratio as follows:

$$Probability\ of\ floodzone = \frac{odds}{1 + odds}$$

By performing these calculations, the result from the logit model are easily interpreted. By calculating the probability that an area is within a flood zone before and after land subsidence, I can estimate how a change in land surface elevation due to land subsidence can increase the expected damages from flooding.

Observations for the independent variables in the dataset are created using the "fishnet" tool in ArcGIS to create 300m by 300m squares throughout the study region, as described in the spatial interpolation of Chapter 2. This yields 47,911 observations. For each 300m cell the dataset describes elevation in meters, percent slope, distance from water in meters, and a dummy variable representing land cover data from the National Land Cover Database (NLCD). I merge

land cover classes from the NLCD into five classes as described in Table 3: forest, water, shrub, wetland, and developed.[15] The summary statistics for the dataset are in Table 4.

Table 3: Land Cover Class Mapping

Original Class	New Class
Open Water	Water
Developed, Open Space	Developed
Developed, Low Intensity	Developed
Developed, Medium Intensity	Developed
Developed, High Intensity	Developed
Barren Land	Shrub
Deciduous Forest	Forest
Evergreen Forest	Forest
Mixed Forest	Forest
Shrub/Scrub	Shrub
Herbaceous	Shrub
Hay/Pasture	Shrub
Cultivated Crops	Shrub
Woody Wetlands	Wetland
Emergent Herbaceous Wetlands	Wetland

Table 4: Summary Statistics of Explanatory Variables

Variable	Obs	Mean	Std. Dev.	Min	Max
Flood Zone	47911	0.379370082	0.485235342	0	1
Elevation	47911	12.22231347	9.622974177	0	40.61904762
Percent Slope	47911	1.411496255	1.367776693	0	16.78140464
Dist. To Water	47911	2693.94821	2927.311043	0	14072.25522
For	47911	0.172298637	0.377643739	0	1
Water	47911	0.015841873	0.124864863	0	1
Shrub	47911	0.36970633	0.482730177	0	1
Wetland	47911	0.267516854	0.442668812	0	1
Developed	47911	0.174636305	0.379659682	0	1

Multiple specifications of the logit model were run in order to come up with the preferred model for predicting changes in flood zone designation. I hypothesize that elevation plays a major role in determining flood zone designation. First, I estimate three separate logit models, each using a subset of observations that differ based on elevation. One uses observations with an

[15] The mapping used for land cover class is shown in table 3.

elevation between 0 and 10 meters (elevation class 1); the second uses observations with an elevation between 10 and 24 meters (elevation class 2); and the third uses observations with an elevation between 24 and 41 meters (elevation class 3). These classes were chosen based on natural breaks in the histogram of elevations across the study region. These results are shown in tables 5, 6, and 7.

Table 5: Logit Results Elevation Class 1 (0-10 Meters)

Variable	Coef	Std. Error	z	P>z	95% CI
Elevation	-0.37963	0.007399	-51.31	0	-0.39 - -0.37
Percent Slope	1.605445	0.026713	60.1	0	1.55 – 1.66
Dist. To Water	-0.00013	0.0000129	-9.78	0	-0.0002 - -0.0001
For	0.079677	0.077333	1.03	0.303	-0.072 – 0.231
Water	0.975537	0.106136	9.19	0	0.77 – 1.18
Shrub	-0.67527	0.044286	-15.25	0	-0.76 - -0.59
Wetland	0.99849	0.039046	25.57	0	0.92 – 1.08
Constant	0.501335	0.038203	13.12	0	0.43 – 0.58

Table 6: Logit Results Elevation Class 2 (10-24 Meters)

Variable	Coef	Std. Error	z	P>z	95% CI
Elevation	-0.23569	0.005946	-39.64	0	-0.25 - -0.22
Percent Slope	0.508257	0.016294	31.19	0	0.48 – 0.54
Dist. To Water	3.43E-05	7.04E-06	4.87	0	0.00002 – 0.00005
For	0.569044	0.125074	4.55	0	0.32 – 0.81
Water	0.759938	0.320566	2.37	0.018	0.13 – 1.38
Shrub	0.560245	0.123452	4.54	0	0.32 – 0.80
Wetland	2.324166	0.130696	17.78	0	2.07 – 2.58
Constant	0.960299	0.148315	6.47	0	0.67 – 1.25

Table 7: Logit Results Elevation Class 3 (24-41 Meters)

Variable	Coef	Std. Error	z	P>z	95% CI
Elevation	-0.28119	0.039509	-7.12	0	-0.36 - -0.20
Percent Slope	0.826834	0.062505	13.23	0	0.70 – 0.95
Dist. To Water	-0.00025	4.25E-05	-5.83	0	-0.0003 - -0.0002
For	-0.44099	0.626051	-0.7	0.481	-1.67 – 0.79
Water[16]	(omitted)				

[16] The independent variable *water* was omitted in the third elevation class due to perfect correlation with the dependent variable *flood zone*.

Shrub	-0.23821	0.616793	-0.39	0.699	-1.45 – 0.97
Wetland	0.106389	0.76654	0.14	0.89	-1.40 – 1.61
Constant	2.998974	1.240605	2.42	0.016	0.57 – 5.43

Based on tables 5 through 7, the estimated coefficient for elevation differs by class and is statistically significant in each case. What is more interesting from an economic perspective is the marginal effect that a change in elevation has on the probability of a location being within a flood zone. These results are in table 8. For areas located in elevation class 1, as elevation increases by 1 meter the probability that an area is in a flood zone decreases by 6.2%; in class 2 the probability increases by 3.3%; and in class 3 the probability increases by only 0.5%. These results suggest that home values in areas with lower land elevation are more likely to be affected by changes in flood risk due to land subsidence.

Table 8: Marginal Effects of Elevation Per Elevation Class

Elevation Class	Variable	Coef	Std. Error	z	P>z
1	Elevation	-0.06234	0.0010	-64.87	0
2	Elevation	-0.03309	0.0007	-47.49	0
3	Elevation	-0.00525	0.0008	-6.57	0

Separating the data by elevation classes has the advantage of allowing all slope parameters in the model to differ by elevation class. However, the specification of different models by elevation class complicates the mathematical simulation model because it requires the dataset to be divided into three different groups based on the elevation class, as well as the addition of two logit models. To simplify the simulation, I consider simplifying the logit model based on three different specifications: the first includes only dummy variables for elevation class; the second includes interaction terms between elevation and the elevation class (allowing the slope coefficient on elevation to differ by class); and the third includes both intercept and slope shifters for elevation class. The full results from the logit estimates for each of these specifications are in tables 9 through 11.

Table 9: Logit Results Elevation Class Dummy Variables Only

fz	Coef.	Std. Err.	z	P>z	95% Conf.	Interval
elev	-0.2913824	0.0049472	-58.9	0	-0.3010788	-0.281686
pctslope	0.91583	0.0144214	63.5	0	0.8875646	0.9440955
distowater	0.0000117	6.57E-06	1.78	0.075	-1.19E-06	0.0000245
forest	-0.4225131	4.95E-02	-8.53	0	-0.5196083	-3.25E-01

water	0.901332	0.0989822	9.11	0	0.7073305	1.095334
shrub	-0.5430235	0.0378669	-14.34	0	-0.6172412	-0.4688057
wetland	0.933704	0.0348938	26.76	0	0.8653134	1.002095
class_1	-1.62318	0.1391871	-11.66	0	-1.895982	-1.350379
class_2	-0.0620596	0.1086341	-0.57	0.568	-0.2749785	0.1508594
_cons	2.075856	0.1536889	13.51	0	1.774632	2.377081

Table 10: Logit Results Interaction between Elevation and Elevation Class Only

fz	Coef.	Std. Err.	z	P>z	95% Conf.	Interval
elev	-0.2404621	0.0041458	-58	0	-0.2485878	-0.2323364
pctslope	0.9257188	0.0142399	65.01	0	0.8978091	0.9536286
distowater	0.0000115	6.51E-06	1.76	0.078	-1.29E-06	0.0000242
forest	-0.3595285	0.0491857	-7.31	0	-0.4559308	-0.2631263
water	0.8609032	0.1015265	8.48	0	0.6619149	1.059891
shrub	-0.5028001	0.0378957	-13.27	0	-0.5770743	-0.428526
wetland	0.973172	0.0353527	27.53	0	0.9038819	1.042462
elev_class_1	-0.0946486	0.0062796	-15.07	0	-0.1069564	-0.0823407
elev_class_2	0.0258988	0.0038118	6.79	0	0.0184279	0.0333698
_cons	0.626772	0.0355495	17.63	0	0.5570963	0.6964477

Table 11: Logit Results Elevation Dummy and Interaction between Elevation and Elevation Class

fz	Coef.	Std. Err.	z	P>z	95% Conf.	Interval
elev	-0.2613512	0.0408031	-6.41	0	-0.3413237	-0.1813786
pctslope	0.921511	0.0143904	64.04	0	0.8933063	0.9497157
distowater	0.000012	0.00000655	1.83	0.067	-0.000000859	0.0000248
forest	-0.3940103	0.0495406	-7.95	0	-0.4911081	-0.2969125
water	0.8182273	0.0996945	8.21	0	0.6228296	1.013625
shrub	-0.532199	0.0380642	-13.98	0	-0.6068035	-0.4575946
wetland	0.9692225	0.0353992	27.38	0	0.8998414	1.038604
class_1	-0.6492757	1.102809	-0.59	0.556	-2.810741	1.51219
class_2	0.18235	1.107707	0.16	0.869	-1.988716	2.353416
elev_class_1	-0.0601944	0.041287	-1.46	0.145	-0.1411154	0.0207266
elev_class_2	0.0050153	0.0413092	0.12	0.903	-0.0759493	0.0859799
_cons	1.208827	1.102841	1.1	0.273	-0.9527011	3.370356

Because my primary interest is in predicting damages from land subsidence, I use out-of-sample predictive ability to choose among these three specifications. To do so, I withhold 10% of the observations from the sample used to estimate the model coefficients displayed in tables 9-11. I then use these estimated coefficients to predict the likelihood that the excluded model cells

fall within a flood zone. As shown in table 12, the out-of-sample predictive ability of these three model specifications is similar.

Table 12: Accuracy Test Results

Model	Tested	Correct	Pct. Correct
Dummy	4760	3769	79.18%
Interaction	4831	3784	78.33%
Dummy and Interaction	4840	3805	78.62%

Given the similar performance of these three specifications, I proceed with the first, and simplest specification that uses only dummy variables for elevation class. In addition to its simplicity, this model also has the highest accuracy at predicting the presence of a flood zone (by a small margin). Furthermore, this model had the expected signs for elevation class 1 and elevation class 2. Both of these signs are negative, indicating that these two classes are more likely to be in a flood zone than areas located within the highest elevation class. To calculate the coefficients for the simulation model, the final estimation uses 47,748 observations in the dataset. These logit results are in table 13. The marginal effects for this specification are in table 14.

Table 13: Final Estimated Coefficients from Logit Model

fz	Coef.	Std. Err.	z	P>z	95% Conf.	Interval
elev	-0.291182	0.0046949	-62.02	0	-.3003837	-.28198
pctslope	0.9165991	0.0137029	66.89	0	.8897419	.9434563
distowater	0.0000128	6.25E-06	2.04	0.041	5.31E-07	.000025
forest	-0.413128	0.0469153	-8.81	0	-.50508	-.3211755
water	0.8978904	0.0940131	9.55	0	.7136281	1.082153
shrub	-0.548274	0.0359709	-15.24	0	-.6187753	-.4777719
wetland	0.9323832	0.0330877	28.18	0	.8675325	.9972339
class_1	-1.590992	0.1324511	-12.01	0	-1.850591	-1.331392
class_2	-0.02281	0.1033896	-0.22	0.825	-.2254497	.1798302
_cons	2.036011	0.1462346	13.92	0	1.749397	2.322626

Table 14: Marginal Effects of Independent Variables in Final Model

	dy/dx	Std. Err.	z	P>z	95% Conf.	Interval
elev	-0.04236	0.000568	-74.57	0	-0.04348	-0.04125
pctslope	0.133351	0.001605	83.07	0	0.130204	0.136497
distowater	1.86E-06	9.10E-07	2.05	0.041	7.76E-08	3.64E-06
forest	-0.0601	0.0068	-8.84	0	-0.07343	-0.04678

water	0.130629	0.013619	9.59	0	0.103936	0.157321
shrub	-0.07977	0.005175	-15.41	0	-0.08991	-0.06962
wetland	0.135647	0.004649	29.18	0	0.126535	0.144759
class_1	-0.23146	0.019074	-12.14	0	-0.26885	-0.19408
class_2	-0.00332	0.01504	-0.22	0.825	-0.0328	0.02616

The results in table 14 indicate that locations in elevation class 1 are 23.1% more likely to be in a flood zone than cells in elevation class 3 and observations in class 2 are 0.33% more likely to be in a flood zone than cells in class 3. Also, as elevation decreases by 1 meter, the chance of being located within a flood zone increases by 4.2%. In the next chapter, these results are used to simulate changes in flood zones due to predicted land subsidence across the study region.

To estimate the expected loss from this increased probability of flooding I modified the expected utility function from Nicholson and Snyder (2012) based on work by Michael (2007). This formula looks at the probability that each cell is located within a flood zone and determines the expected loss depending on the total home values in each cell. The expected loss is equal to the product of the change in risk of flooding multiplied by the average home value within each cell, the number of homes within each cell, and the percent of home value loss from being within a flood zone based on the hedonic literature.

$$Expected\ Loss_i = \Delta Risk_i * Home\ Value_i * Number\ of\ Homes_i * Percent\ Loss$$

This expected loss value will be used to estimate the total damages from pumping at each site. These results can then be compared between each pumping site in order to see if the location of pumping affects the amount of damage from land subsidence.

CHAPTER 4. SIMULATED POLICY RESULTS

By estimating the increased risk of flooding from land subsidence I am able to quantify the monetary damages that home owners could face from this increased risk. In order to estimate these damages I rely on the hedonic pricing literature. By combining the pumping cost externality with the increased flood risk associated with land subsidence I am able to estimate the magnitudes of two types of groundwater pumping damages, namely the pumping cost externality and the loss in property values due to land subsidence (henceforth referred to as the "subsidence externality" for brevity). This chapter examines how these results can potentially be used by policy makers to inform future groundwater pumping restrictions.

The mathematical simulation presented in Chapter 3 calculates the internal and external marginal damages associated with increased pumping costs and flood risk due to groundwater pumping. In order to estimate the total marginal damages from pumping within a single cell, these values are summed. These damage estimates can then be used to create a surface of marginal damages. This surface shows how the damages from a unit of pumping differ across space due to aquifer characteristics as well as the location and value of homes. In this chapter, I first discuss an economic interpretation of this marginal damage surface that can be used to extract policy recommendations from the mathematical simulation model. I then show the baseline results from initial simulations with the model, and finally show how subsidence and subsidence damages vary when different groundwater pumping policies are implemented.

4.1. Policy Interpretation

By accounting for the additional damages that groundwater extraction can cause on communities due to land subsidence, a more economically efficient allocation of resources can be reached. Because there has been very little research looking at how future pumping will affect land subsidence, current pumping schedules are designed with little or no thought towards limiting the long-term damages associated with land subsidence. By taking into account the cost of increased flood risk due to land subsidence, policies can induce an economically efficient quantity of pumping by taking into account the full cost of groundwater extraction.

4.2. Baseline Subsidence Damages

The baseline model simulates pumping at 10 randomly selected sites spanning the study region and for a pumping duration of 10 years. The location of these pumping areas is in figure 8. The

pumping sites are numbered from low subsidence damages to high subsidence damages across the study region (as shown in Figure 8). The pumping rate for each site is held constant in order to see how the marginal damages from pumping compare across the region. Results from this simulation are illustrated in Figure 9 and shown in tables 15 through 17. The expected damages from an increase in flood risk are varied over the range of estimates in the economic literature, from 2.3% to 11.3% of home values, to yield a range of marginal damages. The lower and upper bounds on marginal subsidence damages using these estimates are presented in tables 15-17. In order to investigate if damages from groundwater pumping vary with the duration of pumping, the model is run over three different time periods. The original model simulates pumping over a 10-year period (table 15), the second version extended this period out to 50 years (table 16), and the final simulation takes place over 100 years (table 17).

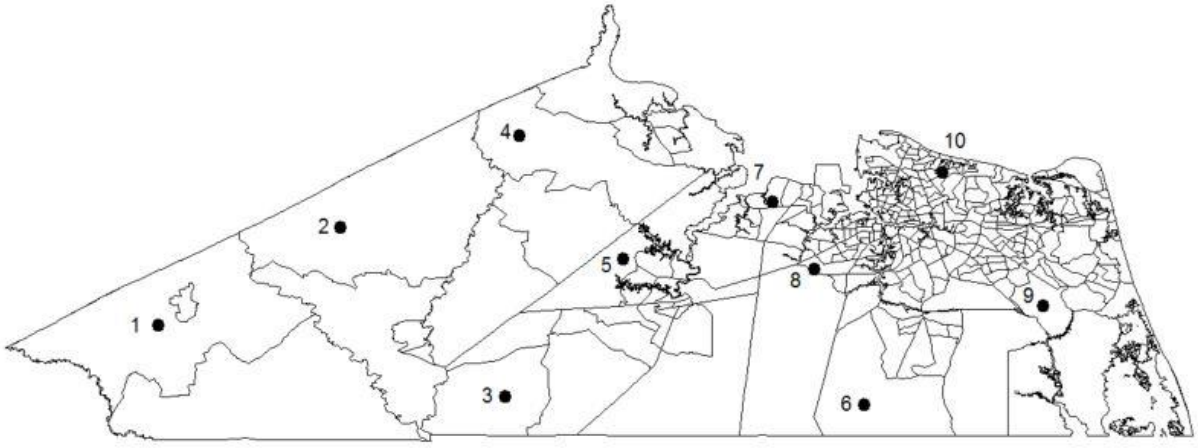

Figure 8: Location of Pump Sites in Relation to Census Tract

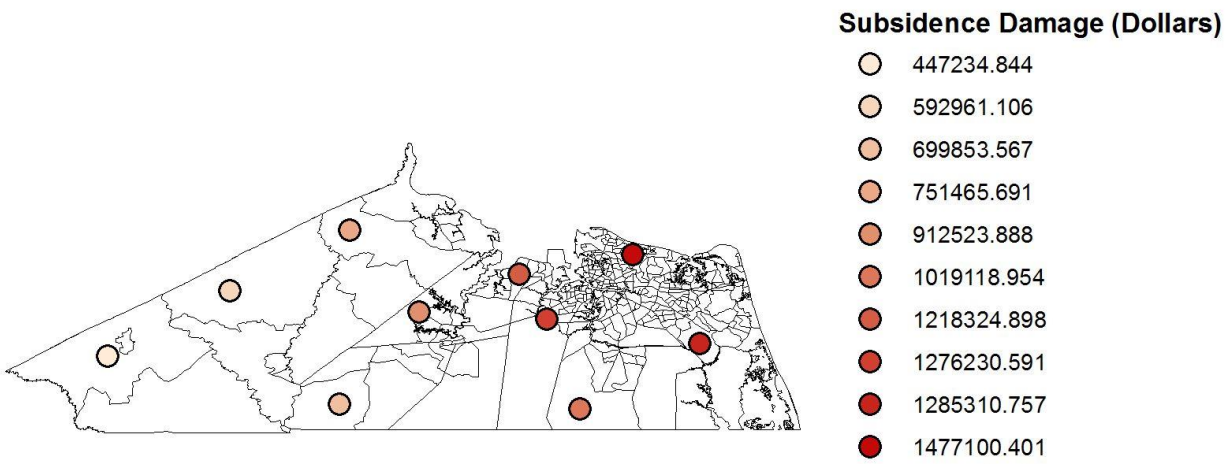

Figure 9: Lower Bound Subsidence Damages after 10 Years of Pumping at Each Site

Table 15: Total Subsidence Damage from Increased Flood Risk after 10 years of Pumping

Pump Site	Total Subsidence Damage Lower Bound 10 years	External Subsidence Damage Upper Bound 10 years
1	$447,234.84	$2,197,284.23
2	$592,961.11	$2,913,243.69
3	$699,853.57	$3,438,411.01
4	$751,465.69	$3,691,983.61
5	$912,523.89	$4,483,269.54
6	$1,019,118.95	$5,006,975.73
7	$1,218,324.90	$5,985,683.20
8	$1,276,230.59	$6,270,176.38
9	$1,285,310.76	$6,314,787.63
10	$1,477,100.40	$7,257,058.49

Table 16: Total Subsidence Damage from Increased Flood Risk after 50 years of Pumping

Pump Site	Total Subsidence Damage Lower Bound 50 years	Total Subsidence Damage Upper Bound 50 years
1	$860,426.46	$4,227,312.60
2	$1,006,144.64	$4,943,232.34
3	$1,113,032.62	$5,468,377.65
4	$1,164,635.19	$5,721,903.31
5	$1,325,686.08	$6,513,153.34
6	$1,432,276.97	$7,036,839.02
7	$1,631,457.00	$8,015,419.16
8	$1,689,366.25	$8,299,929.84
9	$1,698,450.48	$8,344,561.03
10	$1,890,215.22	$9,286,709.54

Table 17: Total Subsidence Damage from Increased Flood Risk after 100 years of Pumping

Pump Site	Total Subsidence Damage Lower Bound 100 years	Total Subsidence Damage Upper Bound 100 years
1	$1,038,370.79	$5,101,560.85
2	$1,184,085.48	$5,817,463.43
3	$1,290,971.52	$6,342,599.22
4	$1,342,569.97	$6,596,104.65
5	$1,503,617.71	$7,387,339.16
6	$1,610,206.79	$7,911,015.97
7	$1,867,286.42	$9,174,059.38
8	$1,876,372.40	$9,218,699.18
9	$1,909,375.64	$8,889,541.19
10	$2,068,126.39	$10,160,797.99

The biggest takeaway from the simulations is that while the extent and location of subsidence vary widely depending on where pumping takes place, the damages occur in the same locations. The areas that suffer the greatest damage are located near the ocean, the Chesapeake Bay, or along river and stream banks. While damages may occur in the same locations independent of where pumping occurs, the magnitude of damages in those locations varies significantly. In the baseline case, the pumping site that creates the least external damages from increased flood risk is located farthest from the coast in the western portion of the study region (site 1 shown in figure 8). Moving from the western border of the study region toward the east, marginal subsidence damages grow significantly, reaching their highest levels in the northeastern coastal portion of the region (shown in figure 9). Table 15 shows that over a 10 year time horizon of pumping, total expected damages from subsidence range from $0.5-1.5 million for the lower bound to $2.2-7.3 million for the upper bound of subsidence damages. The private subsidence damages from pumping within each of the 10 cells, as well as the combined private and external damages are in Appendix E. As I lengthen time in the simulation, the marginal damages decline. This is shown by the differences in marginal damage estimates in tables 15 (10 years), 16 (50 years), and 17 (100 years). As the time since pumping began increases, the marginal change in head height decreases due to the delayed flow of groundwater through the aquifer system.

4.3. Baseline Pumping Damages

Table 17 establishes a range of total marginal subsidence damages for a 100-year period that varies between $1 million and $10.1 million, depending on the location of the pumping site and

the property value loss from a change in flood zone designation. This section estimates the pumping cost externality due to a decrease in groundwater head. This externality is much larger in magnitude than the one-time loss in property values from land subsidence ($1-$10.1 million versus $28-$57 million). The external pumping damage estimates are in table 18, as well as figure 10. What is striking when table 18 is compared with the subsidence externality estimates from the previous section is that while the subsidence externality varies substantially across space, the pumping cost externality is relatively homogeneous. This suggests that the change in head height has less to do with the location of pumping and more to do with the amount of water extracted from the aquifer. The way that I am using the Theis Equation, the primary factor driving changes in head height is the distance of each cell from the pumping site (other factors such as transmissivity and storativity are held constant across the study region). This increased cost applies to each additional unit of water pumped in the region in all future periods, so this damage is discounted into perpetuity. This explains why the damages occurring from an increased in pumping height are significantly larger than the expected damages due to an increase in flood risk, which is a one-time cost to homeowners.

Table 18: Total Damages from Increased Pumping Height

Pump Site	Total Pumping Damages 10 years	Total Pumping Damages 50 years	Total Pumping Damages 100 years
1	$28,699,137.42	$48,758,969.59	$57,398,274.83
2	$28,699,134.28	$48,758,971.24	$57,398,268.55
3	$28,699,140.07	$48,758,971.08	$57,398,270.13
4	$28,699,140.18	$48,758,968.26	$57,398,270.35
5	$28,699,140.23	$48,758,969.32	$57,398,270.46
6	$28,699,139.88	$48,758,975.72	$57,398,269.76
7	$28,699,138.02	$48,758,968.92	$57,398,276.04
8	$28,699,139.02	$48,758,971.53	$57,398,268.04
9	$28,699,135.32	$48,758,967.45	$57,398,270.64
10	$28,699,136.40	$48,758,967.05	$57,398,270.79

Figure 10: Damages from Increased Pumping Height after 10 Years

4.4. Increasing the Pumping Sites

In the baseline case, pumping was simulated in 10 cells randomly selected across the region. The model is scaled up to include 100 pumping sites to see if there is any significant difference in the spatial heterogeneity in the results. Table 19 presents summary statistics for the external subsidence damages from the 10 original pumping sites and the 100 pumping sites. In both cases, results are presented for a pumping duration of 10 years. Figures 11 and 12 illustrate the spatial pattern of the land subsidence externality simulated for 10 and 100 pumping sites. The damages calculated from 100 sites mimic the results from the simulation with 10 sites and are presented here to further emphasize the spatial heterogeneity associated with land subsidence.

Table 19: Summary Statistics 10 Years of Pumping, Lower Bound Subsidence Damages

	10 Pump Sites	100 Pump Sites
Mean	968,012.470	884,793.189
Median	965,821.421	839,324.168
Standard Dev.	342,193.718	290,219.973
Min	447,234.844	371,641.574
Max	1,477,100.401	1,533,775.577
Range	968,0124.697	1,162,134.002

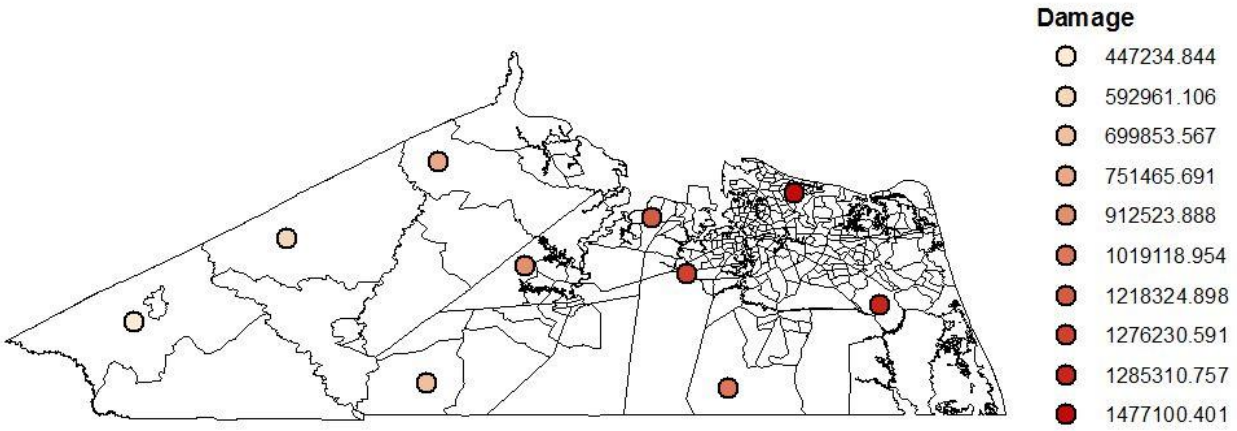

Figure 11: External Subsidence Damages 10 Sites in Dollars

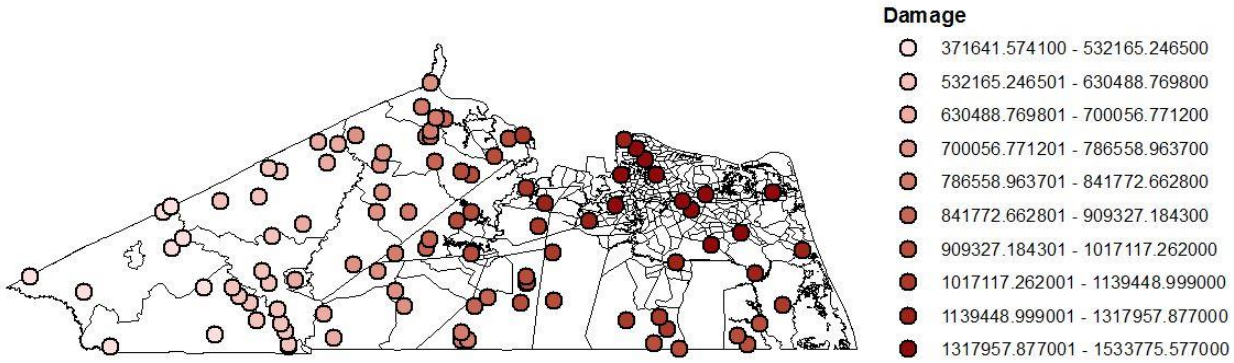

Figure 12: External Subsidence Damages 100 Sites in Dollars

4.5. Policy Limiting Land Subsidence

A policy aimed at limiting land subsidence will prioritize areas with smaller confining units, areas with lower compressibility coefficients, areas with higher storativity values, and areas with higher transmissivity values. If these factors are considered when implementing a new water pumping policy then most pumping would occur in the center of the study region near the Suffolk and Isle of Wight border. According to McFarland (2013), this region has consistently high values of transmissivity. According to my interpolation in Chapter 2, this area also has a relatively thin confining unit thickness. Table 20 and figure 13 show the average total subsidence caused from pumping at each site for 10 years. Focusing on limiting subsidence itself would

result in pumping damages similar to those from pumping site 9 (marked with an "x" in figure 10), with an average total subsidence rate of 6 mm after 10 years of pumping.

Table 20: Average Subsidence in the Study Region

Pump Site	Average Total Subsidence throughout the Study Region in mm After 10 Years of Pumping
1	6.825
2	7.84
3	8.015
4	7.345
5	8.129
6	6.61
7	7.255
8	7.329
9	5.967
10	6.296

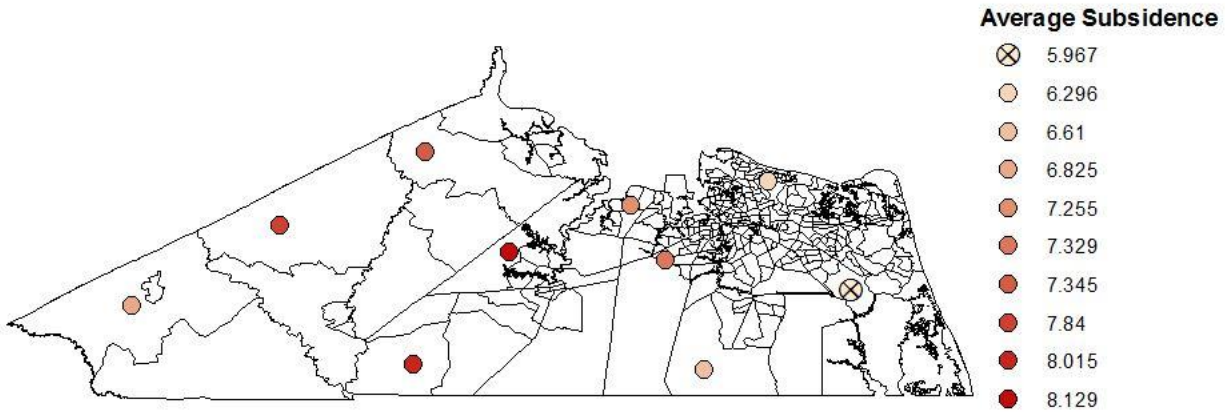

Figure 13: Average Subsidence Rates

If a policy limits each pumping site to creating an average of 6 mm of land subsidence, all other sub-regions would face pumping restrictions. The required restrictions by pumping site are in table 21. Though it is possible to implement pumping restrictions to limit land subsidence, it is difficult administratively to create a policy like the one in table 21 that is specific to each pumper. It is more administratively viable to implement a policy that varies by county. If this

policy the county level pumping reductions required to limit average subsidence to 6 mm are in table 22.

Table 21: Pumping Rates per Site to Reach 6mm of Subsidence after 10 Years

Pump Site	Pumping Rate to Create 6 mm subsidence	Percent of Original Pumping Rate
1	1.35	87.10%
2	1.18	76.13%
3	1.15	74.19%
4	1.25	80.65%
5	1.15	74.19%
6	1.4	90.32%
7	1.25	80.65%
8	1.25	80.65%
9	1.55	100.00%
10	1.48	95.48%

Table 22: Restrictions Placed on Each County to Achieve Desired Subsidence Levels

Municipality	Pumping Rate
Virginia Beach	1.55
Norfolk	1.48
Chesapeake	1.33
Portsmouth	1.33
Suffolk	1.18
Isle of Wight	1.25
Franklin City	1.23
Southampton	1.27

4.6. Policy Limiting the Damages from Land Subsidence

The previous section examines groundwater pumping restrictions based on limiting land subsidence itself. This section considers policies that focus instead on limiting the damages from subsidence. Figures 16 through 25 each illustrate land subsidence (top panel) and the marginal damages from land subsidence (bottom panel) due to pumping at different pumping sites. As shown in figures 16 through 25, the location of land subsidence and the damages from land subsidence follow two different spatial patterns. If you compare the damage models to figure 14, which shows the land cover of the region, it is clear that the majority of damages are in areas of high development. In contrast, comparing the subsidence maps in figures 13 through 22 with figure 15, it is easy to see that subsidence occurs in areas with a thicker confining unit.

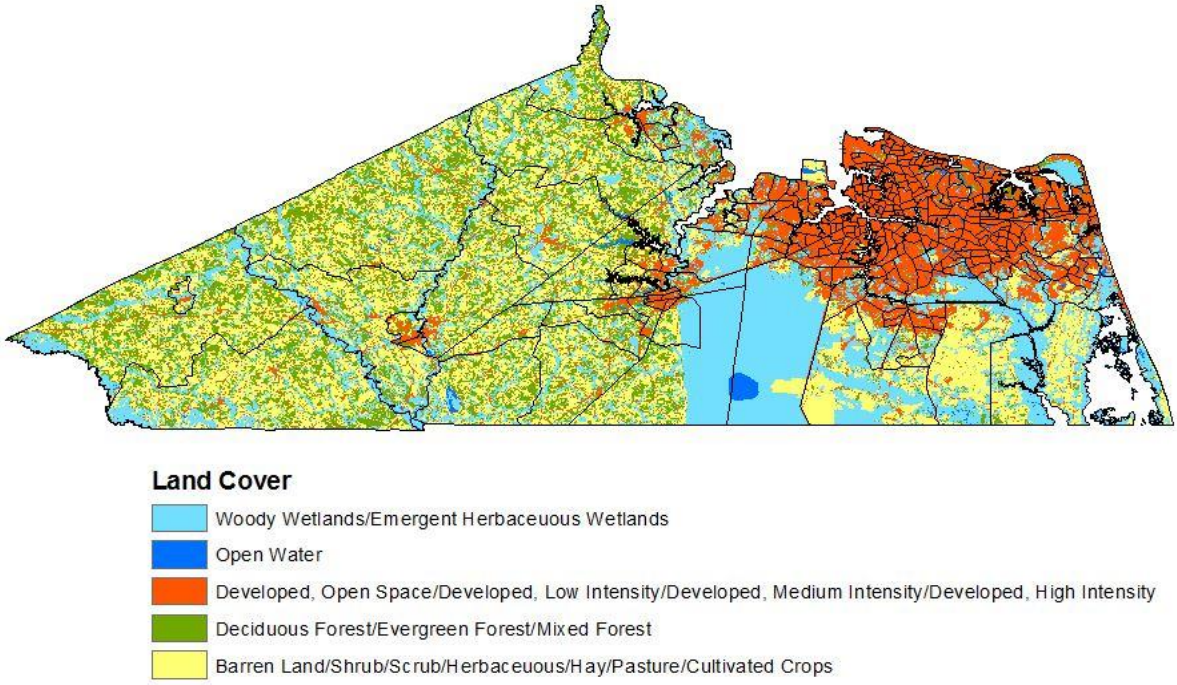

Figure 14: Land Cover Classes

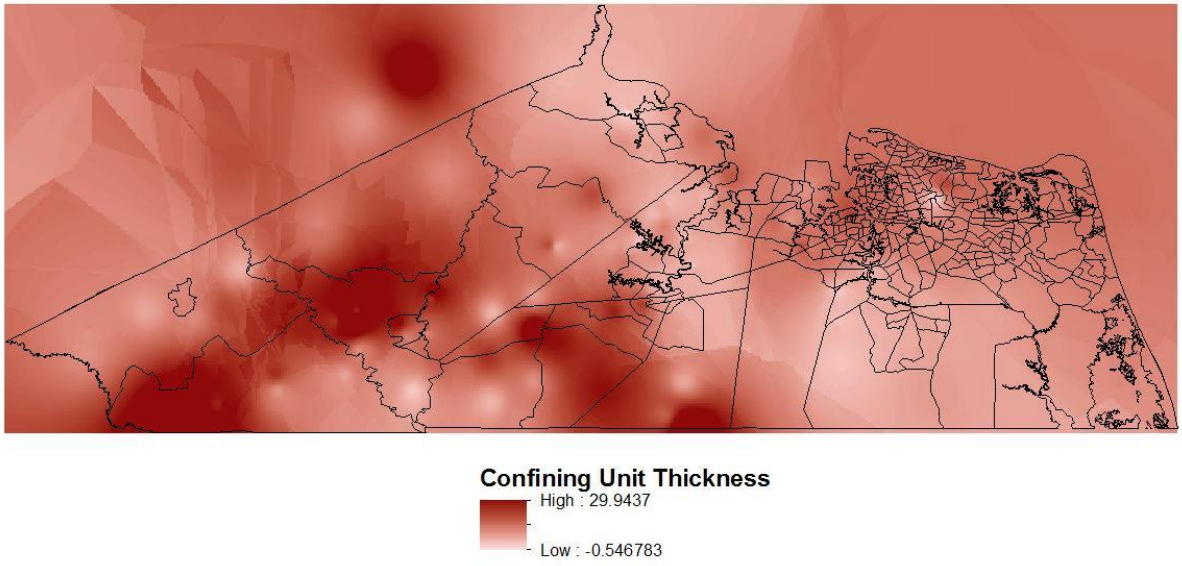

Figure 15: Confining Unit Thickness in Meters

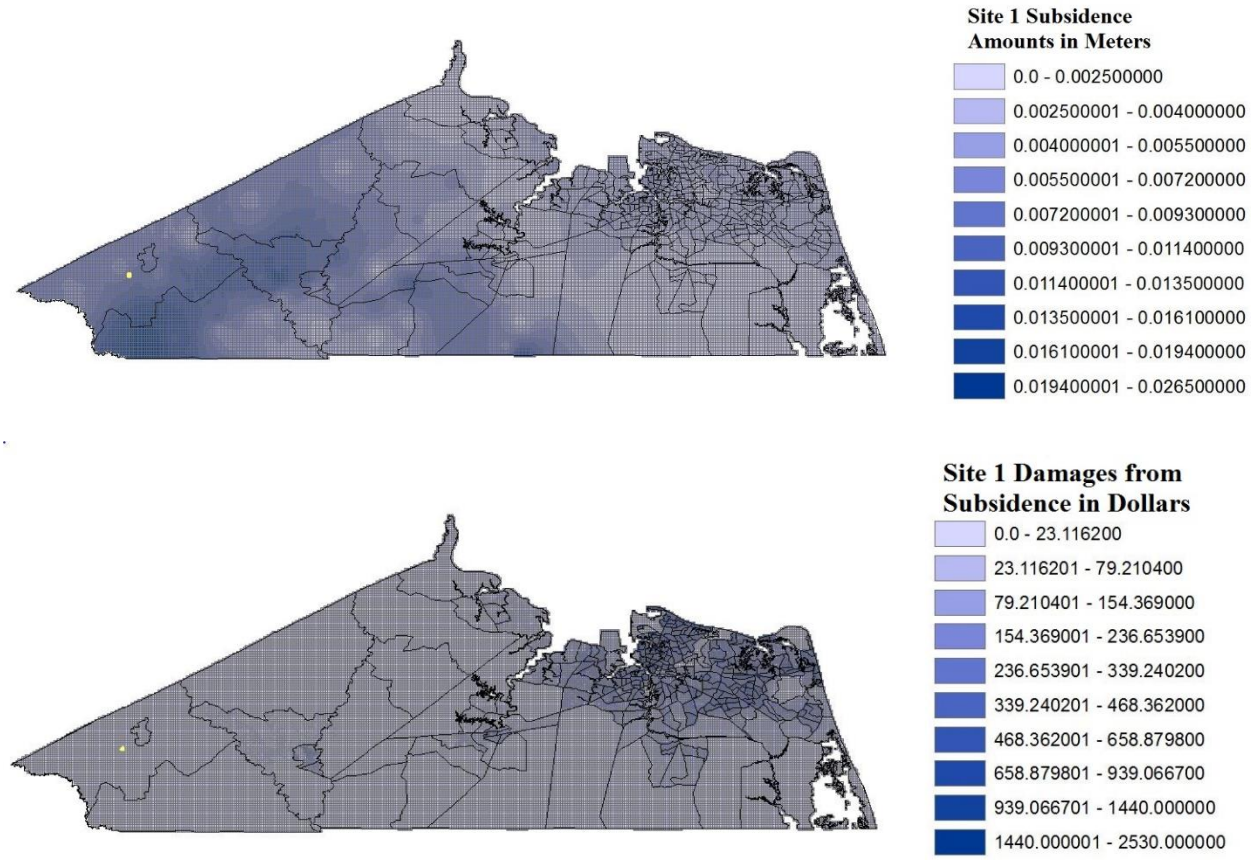

Figure 16: (Top) Location of Subsidence, (Bottom) Location of Subsidence Damages for Pumping Site 1 (in Yellow)

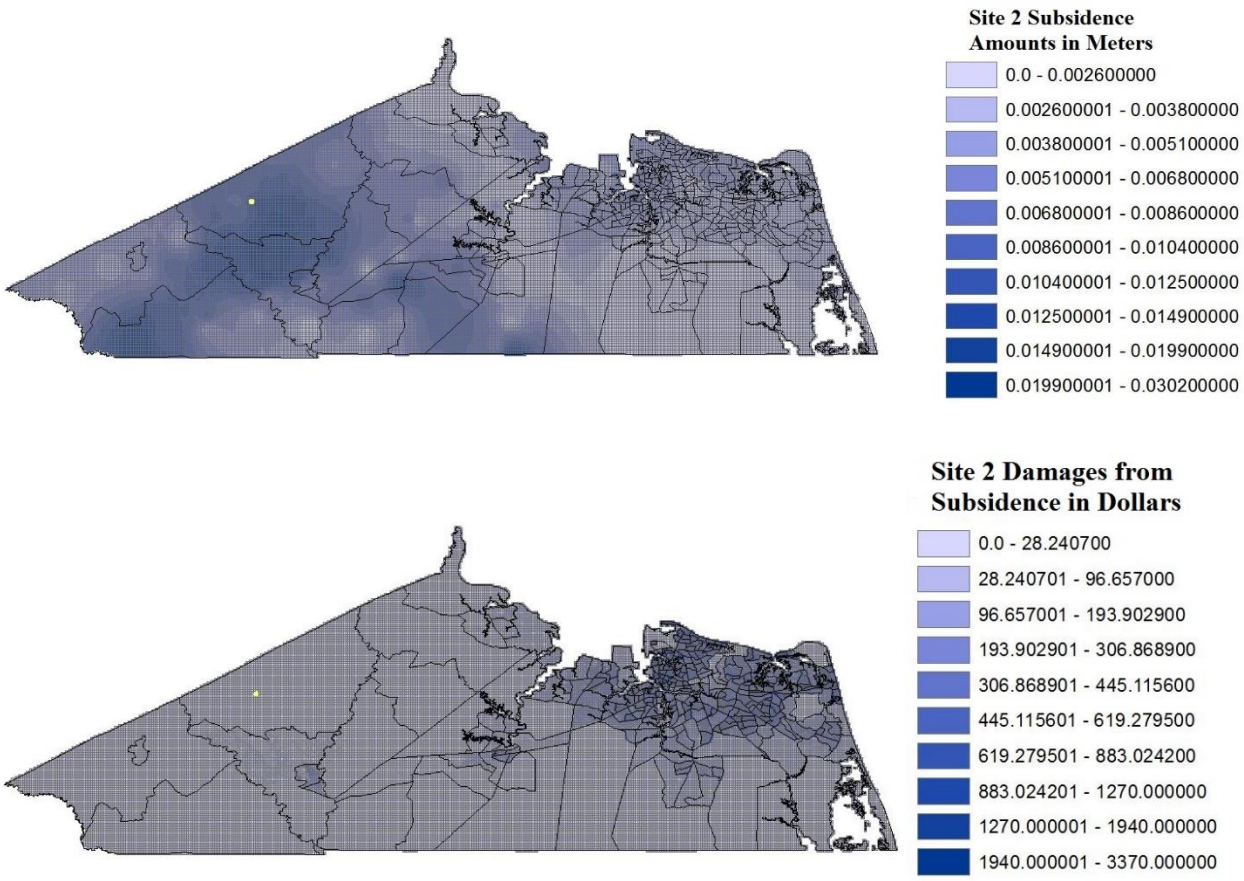

Figure 17: (Top) Location of Subsidence, (Bottom) Location of Subsidence Damages for Pumping Site 2 (in Yellow)

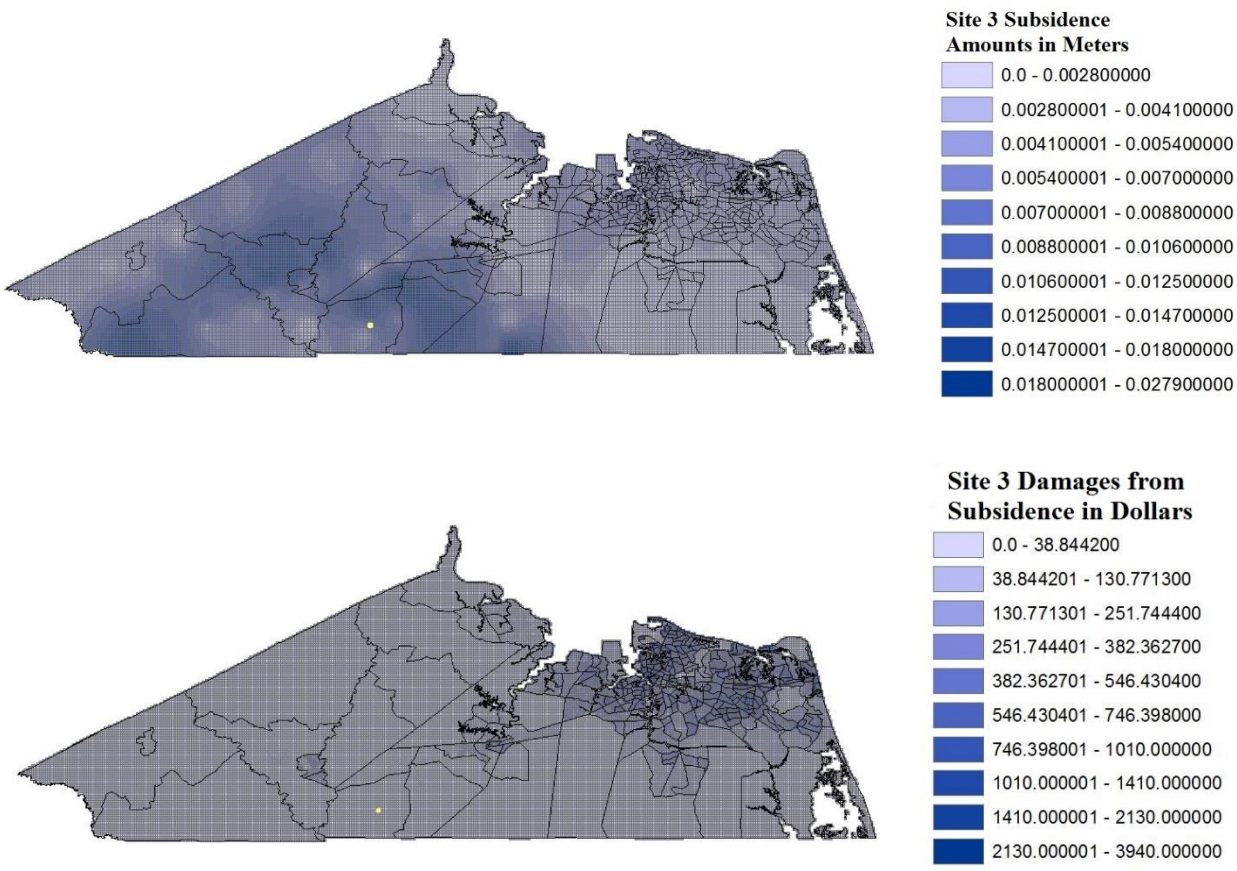

Figure 18: (Top) Location of Subsidence, (Bottom) Location of Subsidence Damages for Pumping Site 3 (in Yellow)

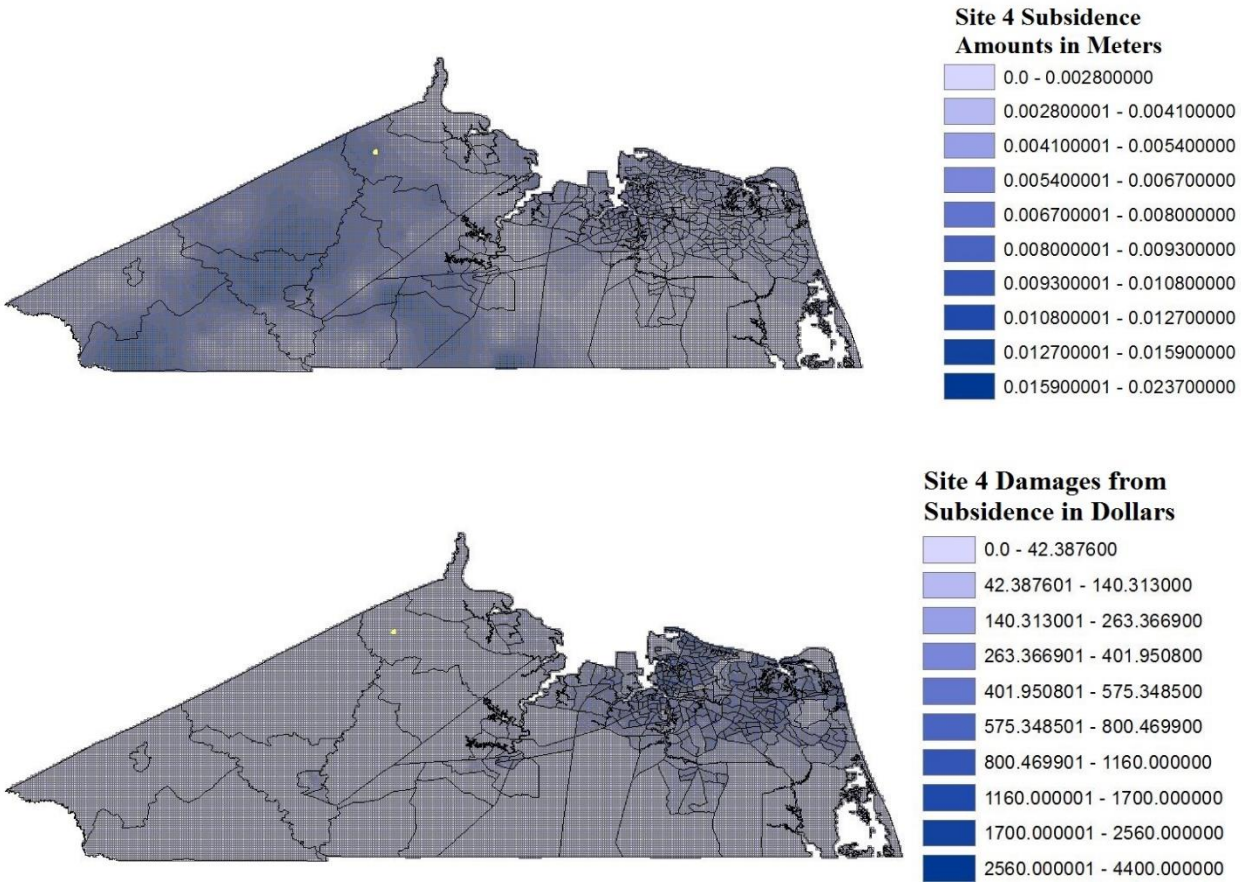

Figure 19: (Top) Location of Subsidence, (Bottom) Location of Subsidence Damages for Pumping Site 4 (in Yellow)

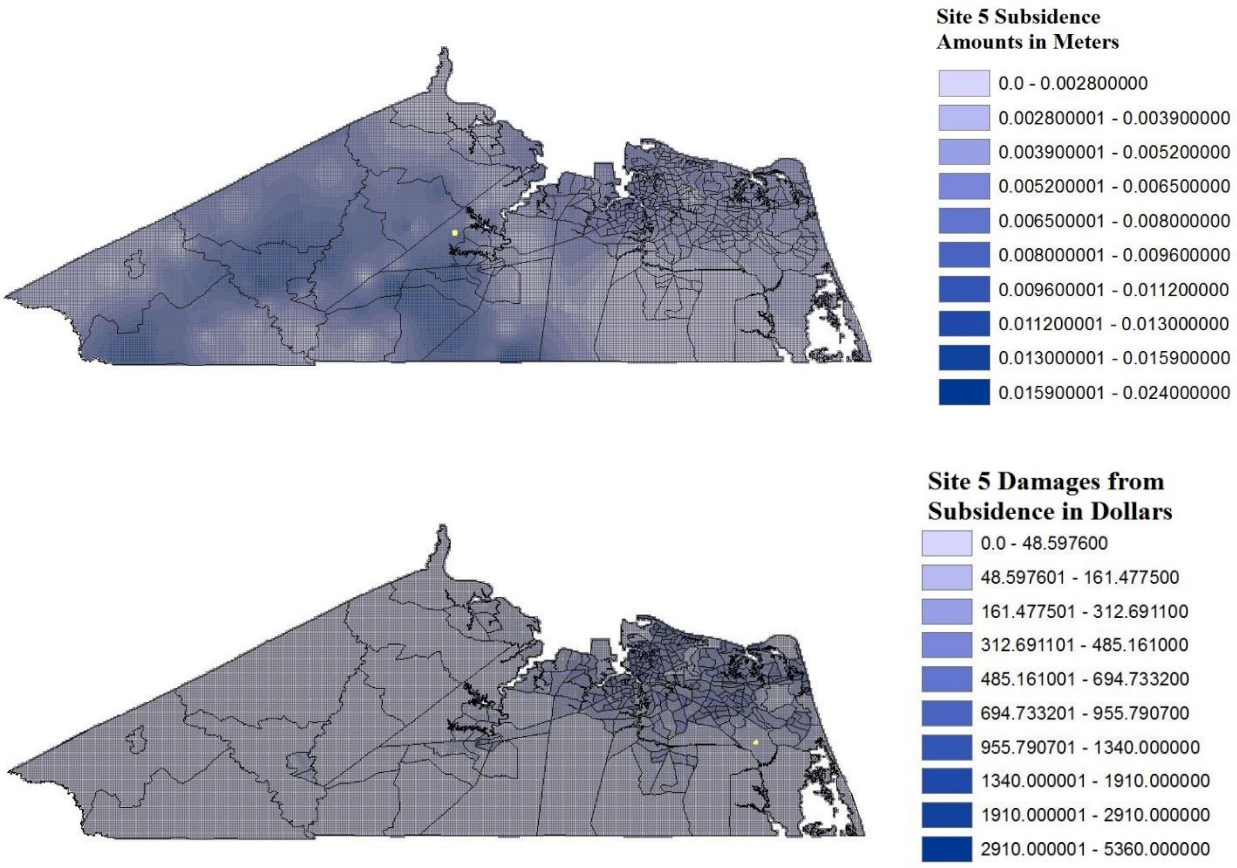

Figure 20: (Top) Location of Subsidence, (Bottom) Location of Subsidence Damages for Pumping Site 5 (in Yellow)

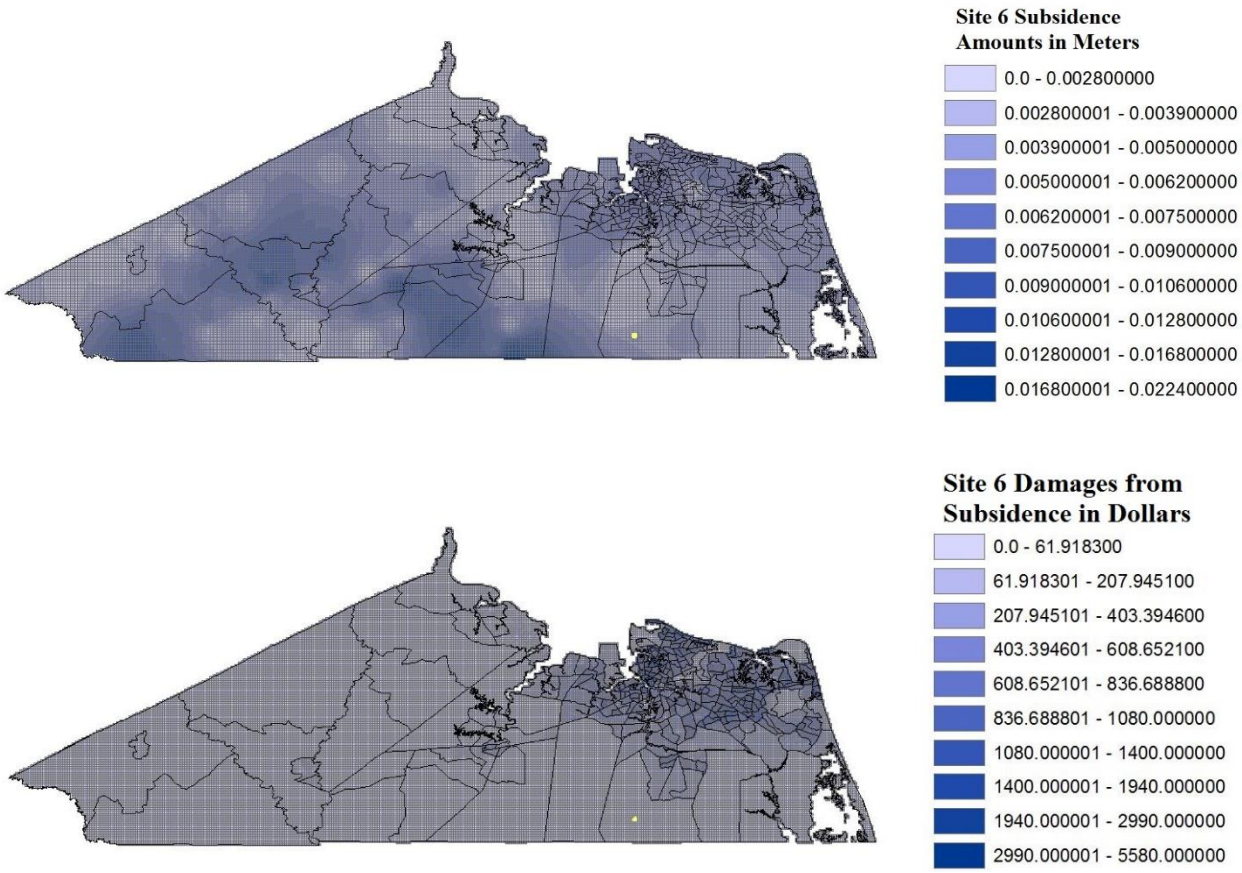

Figure 21: (Top) Location of Subsidence, (Bottom) Location of Subsidence Damages for Pumping Site 6 (in Yellow)

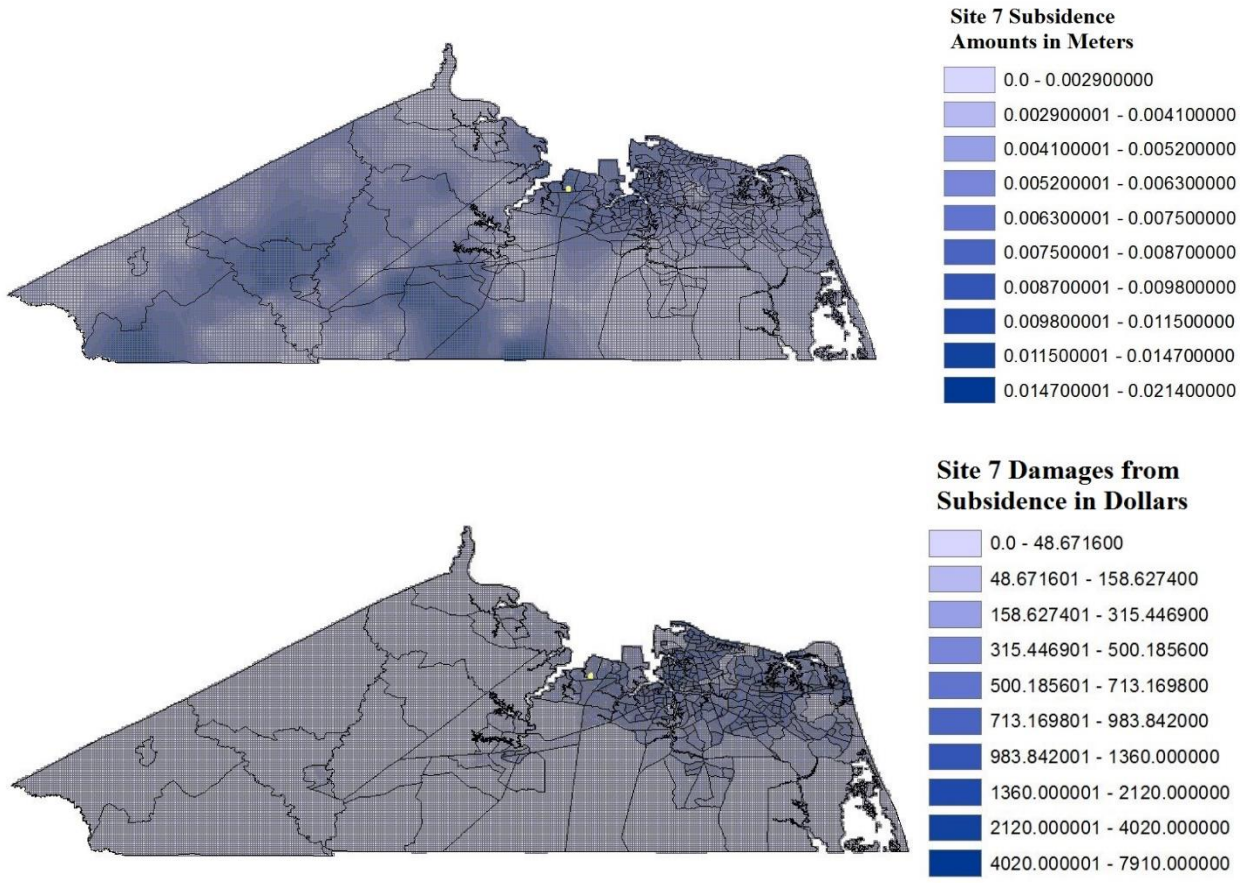

Figure 22: (Top) Location of Subsidence, (Bottom) Location of Subsidence Damages for Pumping Site 7 (in Yellow)

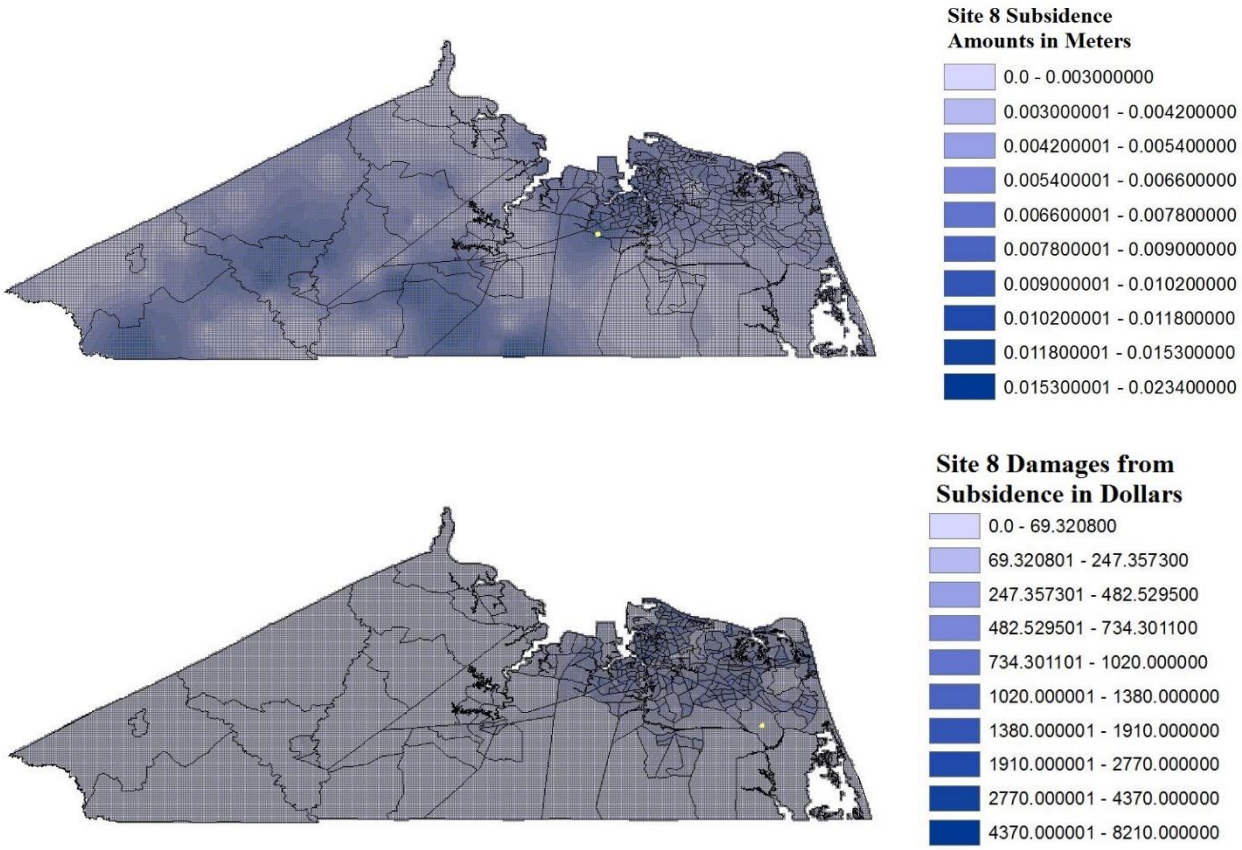

Figure 23: (Top) Location of Subsidence, (Bottom) Location of Subsidence Damages for Pumping Site 8 (in Yellow)

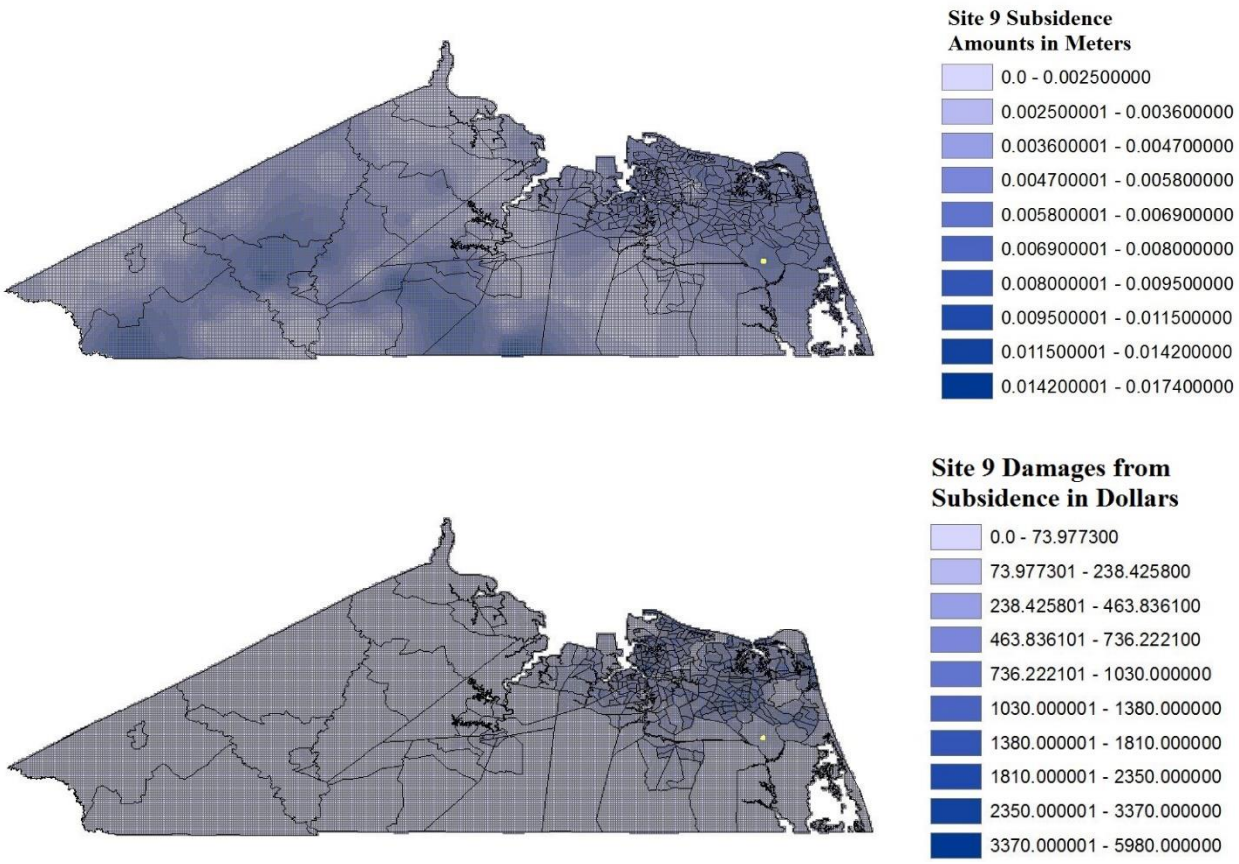

Figure 24: (Top) Location of Subsidence, (Bottom) Location of Subsidence Damages for Pumping Site 9 (in Yellow)

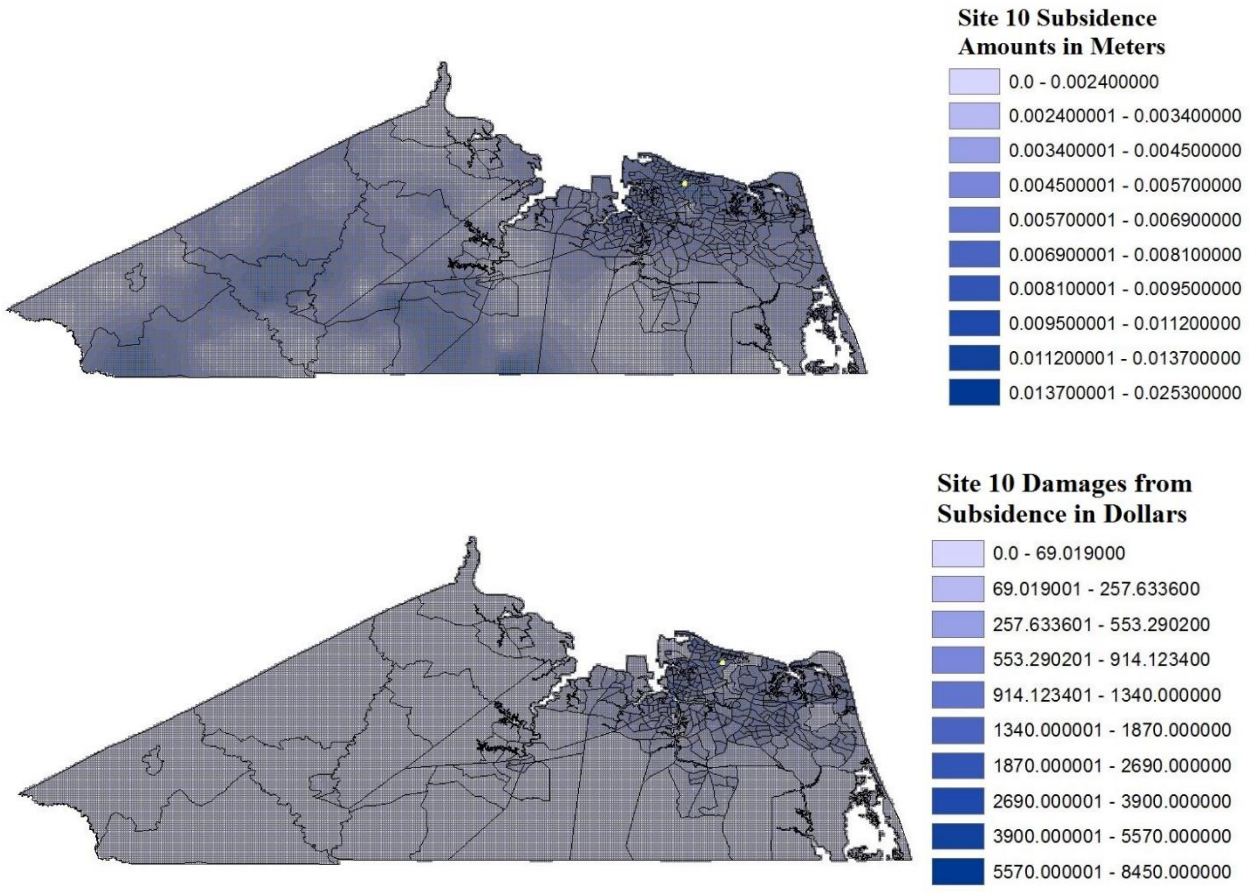

Figure 25: (Top) Location of Subsidence, (Bottom) Location of Subsidence Damages for Pumping Site 10 (in Yellow)

A socially optimal policy will balance the marginal costs and benefits of groundwater extraction, including the marginal external damages associated with land subsidence. Currently, the full cost of groundwater is not accounted for because the damages that are caused by land subsidence are not fully recognized. As demonstrated by Pigou (1938), it is possible to create a tax equal to the marginal external damages from land subsidence and pumping costs that will move current groundwater pumping to an efficient level. Alternatively, a policy that limits pumping in each site such that the marginal damages from pumping are equated across the region would also result in an economically efficient distribution of pumping effort.

With this simulation, I am able to show the significant spatial difference in marginal damages from increased flood risk due to subsidence. With this information, it is possible to

outline how a groundwater pumping policy could be designed to ensure that marginal pumping damages are equated across the region. Because the increased pumping cost due to head height decline is relatively homogeneous throughout the region, it is the spatial difference in the damages from land subsidence that plays the primary role in determining the areas in which groundwater pumping reductions should optimally be prioritized.

With the simulation model developed here, it is not possible to equate marginal pumping damages to find the optimal distribution of pumping across the study region. However, the model can be used to identify the pumping reductions required to limit the total external subsidence damages from each pumping site. Table 15 shows the total subsidence damages from 10 years of pumping. From this table we can see how total damages vary throughout the region.

If policy makers limit subsidence damages to $500,000 over 10 years, pumping rates in all but one site (1) would have to decrease. The results of this policy are shown in table 23. Here we can see that the effect this uniform policy is going to have on each site is very different, with values ranging from a low of 33.68% to a high of 84.03%.

Table 23: Pumping Rates at Which Each Site Causes $500,000 in Subsidence Damages

ID	Pump Rate to Create $500,000 Subsidence Damages	Percent of Original Pump Rate
1	1.726	111.57%
2	1.3	84.03%
3	1.102	71.23%
4	1.025	66.26%
5	0.845	54.62%
6	0.755	48.80%
7	0.633	40.92%
8	0.605	39.11%
9	0.6	38.78%
10	0.521	33.68%

Given that implementing pumping restrictions is administratively costly, it may be more realistic to implement a policy in which pumping reductions are made at the county level. Table 24 outlines the pumping rates that would be allowed in each county to reach the $500,000 damage threshold.

Table 24: County Level Reductions to Achieve $500,000 in Subsidence Damages

Municipality	Pumping Rate
Virginia Beach	0.60

Norfolk	0.52
Chesapeake	0.68
Portsmouth	0.69
Suffolk	0.86
Isle of Wight	1.03
Franklin City	1.13
Southampton	1.51

4.7. Policy Comparison

In figures 26 and figure 27, the site level restrictions from a policy aimed at limiting land subsidence damages are compared with the site level restrictions aimed at liming land subsidence itself. The economically efficient allocation is when the pumping damages are equated across the region as shown in figure 26. The pumping reductions required to equate marginal external damages are greatest in the northeastern corner of the region (in lighter shades) and lowest in the southwestern corner of the region (in darker shades). Figure 27, in contrast, illustrates the pumping reductions required to equate subsidence rates. This policy requires the greatest pumping reductions in the west-central portion of the region, and the smallest pumping reductions in the northeastern corner. The pumping reduction policy illustrated in figure 27 will generate greater economic damages than the policy illustrated in figure 26 because the latter policy allows for more pumping in areas that generate higher marginal damages.

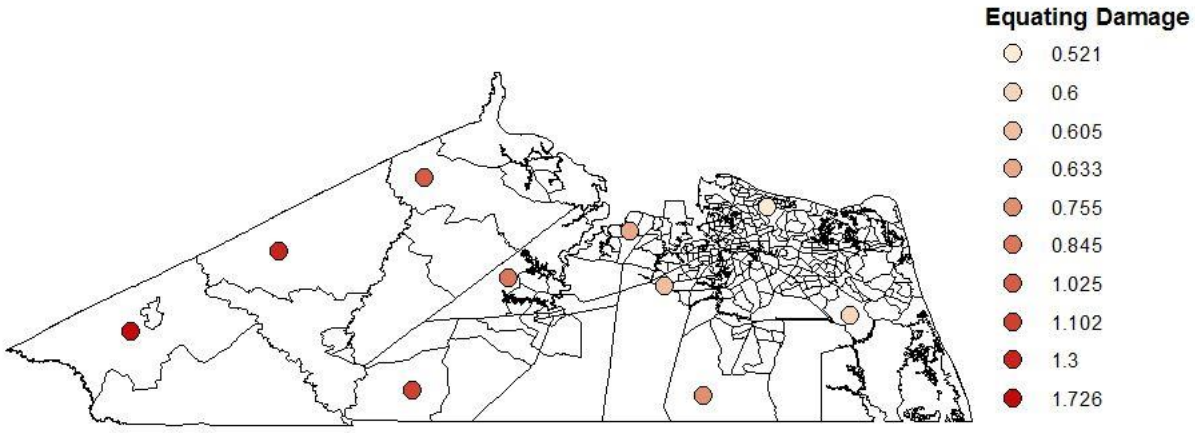

Figure 26: Pumping Rates to Equate Damages

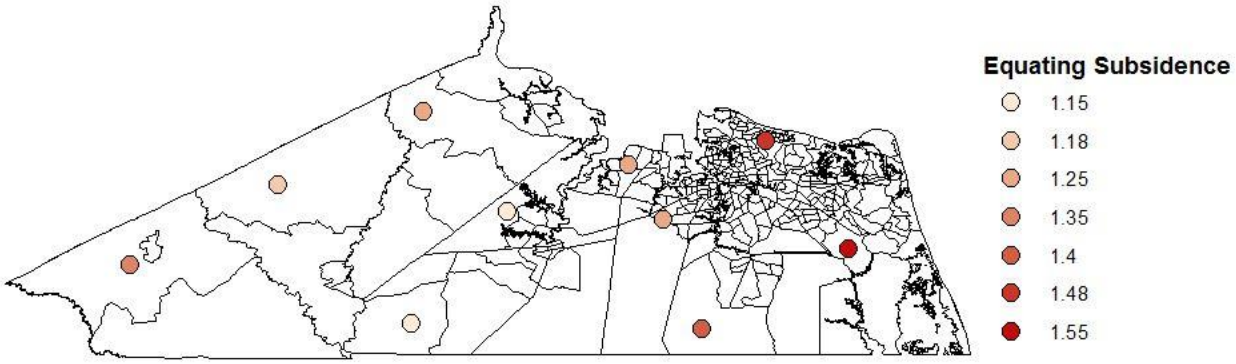

Figure 27: Pumping Rates to Equate Subsidence

CHAPTER 5. CONCLUSIONS AND FUTURE ADVANCEMENT OF THIS STUDY

This study has investigated one of potentially many externalities that can be caused from human interactions with natural resources. Due to the common pool nature of groundwater resources and the physical characteristics of the Potomac Aquifer system in southeastern Virginia, groundwater extraction can create significant economic damages for homeowners. Currently these damages are not internalized by groundwater pumpers, so pumping decisions do not reflect the full social cost of groundwater use. By my estimate, current damages, at minimum, range between $0.4 million and $1.4 million per 1 Mgal/day 10 years after pumping has occurred of pumping. Policy makers need to be aware of these damages and how they vary both spatially and temporally when deciding how to regulate future water projects. The simulation presented here demonstrates that the economic damages from land subsidence vary substantially across space with the density and value of houses, and not necessarily with the physical characteristics that result in the highest rates of land subsidence. Future research and additions to this model are necessary to be able to show how simultaneous pumping at sites across the region affects land subsidence. With this addition, it is possible to create an optimization program to minimize the economic damages from subsidence while meeting current and future water constraints.

Brozovic et al. (2006) shows that from a theoretical framework that by using single-cell hydrologic models may underestimate the pumping externality by orders of magnitude when compared to spatially explicit models. But, when this theoretical framework was applied to an analytical problem it was found that regulators can generate most of the potential savings in total social cost without accounting for spatial heterogeneity (Kuwayama and Brozovic 2013). However, I have shown that while the pumping cost externality creates heterogeneous damages independent of pumping location, when groundwater pumping induced land subsidence is present, a spatially heterogeneous approach to policy can create significant social benefits. Due to the assumption of uniformly distributed housing throughout the study region, the estimated damages from land subsidence are underestimated in this simulation. This provides further evidence that if land subsidence is present, the benefits from a spatially heterogeneous policy are even greater.

These results are subject to a number of caveats. Hydrologic values vary throughout the region, however sensitivity analysis is presented in the following section to investigate the affect

that these values could have on my damage estimates. Land subsidence can cause additional damages other than increasing the flood risk and some of these damages are presented in section 5.2. The final section of this chapter talks about how the subsidence damages calculated in this paper are linear and issues that can arise due to this assumption.

5.1. Limits to Hydrologic Values

In order to create policies that limit the damages from land subsidence, it is important to recognize the physical factors that lead to higher levels of aquifer system compaction. There are two major factors in the simulation that drive subsidence: water level decline and confining unit thickness.[17] Water level decline depends on pumping rates, the duration of pumping, transmissivity of the aquifer, storativity of the aquifer, and the location of pumping. In the simulation model, all of these factors except for the location of pumping are held constant. In Chapter 2, I interpolated the confining unit thickness throughout the study region. With this data I am able to calculate the average confining unit thickness within each cell. This, along with the distance from pumping is the main driver of land subsidence. With more spatially explicit information on storativity and transmissivity in the region, this model could provide more accurate spatial predictions of drawdown. With this information, policy makers would be able to predict, with greater accuracy, the levels of land subsidence caused from pumping aquifers.

In order to test how other physical attributes of the aquifer system affect land subsidence, it is necessary to look at how storativity and transmissivity affect drawdown through the Theis Equation. Storativity and transmissivity vary throughout the region with ranges of 0.0002 to 0.001 and 3000 ft^2/d to 10,000 ft^2/d respectively (McFarland 2013). By holding these constant in the original simulation, I sacrifice accuracy in subsidence measurements. However, McFarland (2013) states that there is no discernable regional trend regarding the values of storativity; large transmissivity values are generally correlated with the predominance of coarse-grained sediments, and small transmissivity values are correlated with increasingly fine-grained sediments. This makes it hard to create accurate spatially heterogeneous assumptions on the physical characteristics of the aquifer system. Inspection of the Theis Equation below, illustrates how both storativity (*stor*) and transmissivity (*trans*) affect drawdown (*draw*).

[17] The subsidence equation also includes confining unit material coefficient of compression, however this is assumed constant in the simulation.

$$draw(N,t) = \frac{pump * \left[-0.9793 * \ln\left(\frac{Dis(N)^2 * stor}{4 * trans * day(t)}\right) - 0.2722\right]}{12.57 * \frac{trans}{864000}}$$

As transmissivity increases, the function inside of the ln operator becomes less negative, all else being equal. This decreases the numerator. At the same time the denominator increases as transmissivity increases. Thus drawdown decreases, which lowers subsidence levels. If policy makers know the transmissivity throughout the region, land subsidence could be limited by decreasing pumping in areas with lower transmissivity rates. As storativity increases, the bracketed function in the numerator becomes more negative, leading to lower drawdown. If policy makers know where areas of higher storativity lie, then subsidence can be reduced by moving pumping into these areas and away from places with lower storativity values. By varying these values within the simulation it is easy to see how vital an accurate measure of spatially explicit values for transmissivity and storativity is.

In table 25 through 27, I show how the estimated lower bound of marginal subsidence damages change with different values of transmissivity and storativity. When looking at these results, it is interesting to note that the change in marginal pumping cost does not change when storativity is changed. This is because storativity acts as a scalar, so both original pumping height and final period pumping height change by the same amount. This is not the case when transmissivity changes. The increased pumping costs are much higher in areas with lower values of transmissivity.

Table 25: Lower Bound Subsidence Damage with Changing Storativity Value from 10 Years of Pumping

Pump Site	Total Subsidence Damage $stor = 0.0002$	Total Subsidence Damage $stor = 0.001$
1	$447,234.84	$34,018.60
2	$592,961.11	$179,752.92
3	$699,853.57	$286,649.83
4	$751,465.69	$338,271.50
5	$912,523.89	$499,336.97
6	$1,019,118.95	$605,936.18
7	$1,218,324.90	$805,167.99
8	$1,276,230.59	$863,070.11
9	$1,285,310.76	$872,146.22
10	$1,477,100.40	$1,063,960.70

Table 26: Lower Bound Subsidence Damage with Changing Transmissivity Value from 10 Years of Pumping

Pump Site	Total Subsidence Damage $trans = 10{,}000$	Total Subsidence Damage $trans = 3{,}000$
1	$447,234.84	$460,436.59
2	$592,961.11	$946,202.80
3	$699,853.57	$1,302,506.54
4	$751,465.69	$1,474,471.60
5	$912,523.89	$2,011,283.40
6	$1,019,118.95	$2,366,588.16
7	$1,218,324.90	$3,030,170.25
8	$1,276,230.59	$3,223,285.94
9	$1,285,310.76	$3,253,689.87
10	$1,477,100.40	$3,892,507.17

Table 27: Total Pumping Damages with Changing Transmissivity Value from 10 Years of Pumping

Pump Site	Total Pumping Damages $trans = 10{,}000$	Total Pumping Damages $trans = 3{,}000$
1	$28,699,137.42	$95,663,788.05
2	$28,699,134.28	$95,663,780.92
3	$28,699,140.07	$95,663,790.22
4	$28,699,140.18	$95,663,783.92
5	$28,699,140.23	$95,663,784.09
6	$28,699,139.88	$95,663,786.27
7	$28,699,138.02	$95,663,783.39
8	$28,699,139.02	$95,663,790.07
9	$28,699,135.32	$95,663,787.74
10	$28,699,136.40	$95,663,787.99

While drawdown from pumping is one factor in causing land subsidence, there are two other major variables that affect the amount of subsidence that occurs. Both confining unit thickness (*cthick*) and compressibility (*c*) of the aquifer confining unit also play major roles in driving land subsidence. In the subsidence formula below, subsidence is linearly dependent on confining unit thickness and compressibility of the confining unit materials.

$$sub(N,t) = fd * g * draw_m * cthick * c$$

Figure 15 shows the estimate of the confining unit shape that was calculated in ArcGIS. I use these estimates to calculate the average confining unit thickness within each cell. This allows the

simulation to account for spatial heterogeneity in the aquifer system shape. If pumping can be moved away from areas with thick confining units, the potential for land subsidence would be minimized. Because confining unit thickness plays a direct role in the amount of land subsidence, further study on the shape of the aquifer in the region could benefit policy makers by allowing them to make more informed decisions when planning for future water projects. If policy makers are aware of the significance that aquifer confining unit thickness plays on land subsidence, then future water use schedules could strike a balance between extraction and subsidence to limit damages.

Compressibility (*c*) also plays a role in driving land subsidence. According to Freeze and Cherry (1979), clay confining units can have a compressibility coefficient ranging from ranging from 10^{-6} to 10^{-8}. This difference is caused by the variable grain size and the ratio of the volume of water to volume of solids. In the original model, the coefficient is constant at 10^{-7}. However, if this value is increased or decreased to the lower and upper measurements for clay, subsidence rates could vary by a magnitude of 10 in either direction, as shown in Tables 28 and 29. The subsidence results mimic the change in compressibility: as the magnitude of c decreases by a power of 10, so does subsidence. The effect on pumping damage is much smaller because the major driver of pumping cost is head height decline. While subsidence rates are taken into account, the actual size of land subsidence is much smaller than the change in head height. If compressibility is known throughout the region, then areas with a lower compressibility coefficient could handle higher rates of drawdown while producing the same amount of subsidence.

Table 28: Lower Bound Subsidence Damage with Changing Compressibility Value from 10 Years of Pumping

Pump Site	Total Subsidence Damage $c = 10^{-6}$	Total Subsidence Damage $c = 10^{-8}$
1	$4,471,936.71	$44,723.87
2	$5,928,539.19	$59,297.13
3	$6,996,957.43	$69,986.86
4	$7,511,275.31	$75,149.86
5	$9,120,529.72	$91,256.93
6	$10,185,897.89	$101,916.97
7	$12,170,204.30	$121,845.07
8	$12,750,660.31	$127,634.16

9	$12,843,489.39	$128,540.22
10	$14,753,068.34	$147,727.05

Table 29: Total Pumping Damages with Changing Compressibility Value from 10 Years of Pumping

Pump Site	Total Pumping Damages $c = 10^{-6}$	Total Pumping Damages $c = 10^{-8}$
1	$27,242,966.81	$28,844,757.48
2	$27,242,962.86	$28,844,754.42
3	$27,242,968.91	$28,844,750.18
4	$27,242,968.33	$28,844,750.36
5	$27,242,967.41	$28,844,750.51
6	$27,242,968.35	$28,844,750.03
7	$27,242,962.02	$28,844,751.62
8	$27,242,968.74	$28,844,749.05
9	$27,242,963.25	$28,844,757.53
10	$27,242,967.72	$28,844,754.17

Other limitations presented by the Thesis Equation are that it assumes an aquifer is homogeneous, isotropic, and confined. It also assumes that the aquifer is flat, and both the top and bottom boundaries are non-leaky. Because the Potomac Aquifer lies just above the basement bedrock, the bottom boundary is non-leaky, however the clay confining unit lying above the aquifer is leaky. Lastly, the Theis Equations assumes that there is only a single well in the region. This does not allow the Theis Equation to be used to estimate drawdown when there are multiple pumpers utilizing the same aquifer.

The formula used to estimate subsidence also presents limitations. In this context, the main variables in the subsidence calculation are drawdown in each cell, as well as the confining unit thickness in each cell. I assume that compressibility of the confining unit is constant throughout the entire region. While compressibility can vary by a magnitude of 100 for the same material, there is very little research looking at how compressibility changes in the natural environment. Most studies looking at compressibility are done in laboratory settings and are hard to recreate outside of a lab. If it is possible to accurately estimate how compressibility varies throughout the study region, it would be possible to create more accurate land subsidence predictions. As seen in all of these cases, physical factors have the potential to affect land subsidence drastically. With additional research looking at the specific values of transmissivity,

storativity, and compressibility within the study region, it would be possible to estimate subsidence rates, and the corresponding damages from subsidence, more accurately. It is an open question, however, to what extent this might empirically influence the estimated magnitude of land subsidence damages, given that these damages are primarily determined by the location and value of housing.

5.2. Other Damages from Land Subsidence

This model is focusing on two major cost associated with groundwater pumping, the first is the increased cost of pumping due to a lowering of head height, and the second is the increase in expected damages from flooding due to land subsidence. However, there are other damages that can be caused by groundwater pumping. Groundwater is said to have *in situ* value or value for being in the ground. By having large deposits of groundwater a region can insulate themselves from the effect of unforeseen disasters such as drought or the contamination of surface water sources. There is monetary value associated with this limited risk of running out of fresh water and each unit of groundwater extracted incurs a cost by limiting future water availability.

Also land subsidence may create other damages by altering wetland and coastal ecosystems, and/or by damaging infrastructure and historical sites (Eggleston and Pope 2013). As land subsides in coastal regions, areas that were once in the tidal zone may now be permanently inundated with water, and areas that were only under water in extreme high tides may become the new tidal zone. This can harm both plant and animal health as well as destroy homes and other built environments. This destruction of infrastructure has been seen in areas such in the San Joaquin Valley in California where land has subsided at rates as high as 13 inches per year (Boxall 2015). This has caused many bridges to almost touch the water they cross. If land subsidence continues at these rates, many bridges and roads will have to be rebuilt in order to remain passable.

Figure 28: The Russell Avenue Bridge in Firebaugh, CA has sunk so much that it is almost touching the water in the canal it crosses (Boxall 2015)

5.3. Linear Damages from Pumping

Another concern with the simulation model presented in this thesis is that the damage function is linear with respect to total pumping. The marginal damages are constant which does not allow me to apply the economic theory that efficiency can be met when marginal damages are equated across all emitters. As total pumping increases, marginal damages should decrease. With a downward sloping marginal damage function, it is possible to equate marginal damages across all pump sites and find the optimal pattern of pumping in the study region, or the one that produces the economically efficient allocation of groundwater. As currently formulated, the model here produces a corner solution in which the allocation of pumping that minimizes the damages from groundwater extraction requires all pumping to occur at site 1. This is the site that generates the least marginal damage as a result of pumping. Of course, it is not practically feasible, and would be quite costly, to pump the region's groundwater from a single site and transport it to the locations where it is consumed.

In order to address this concern, more research is needed on the relationship between groundwater pumping and land subsidence. By using the Theis Equation and the derived form of Darcy's Law, all factors relating groundwater pumping and land subsidence are linear. However it would follow theory that as groundwater pumping increases, land subsidence would begin to decrease, most likely because the confining unit has already subsided to its maximum rate. More investigation is needed on the marginal effects that an increase in expected damages from flooding can cause. With this information it would be possible to acquire pumping rates for each site that can limit total damages.

Appendix A. Interpolation Results: Basement Bedrock

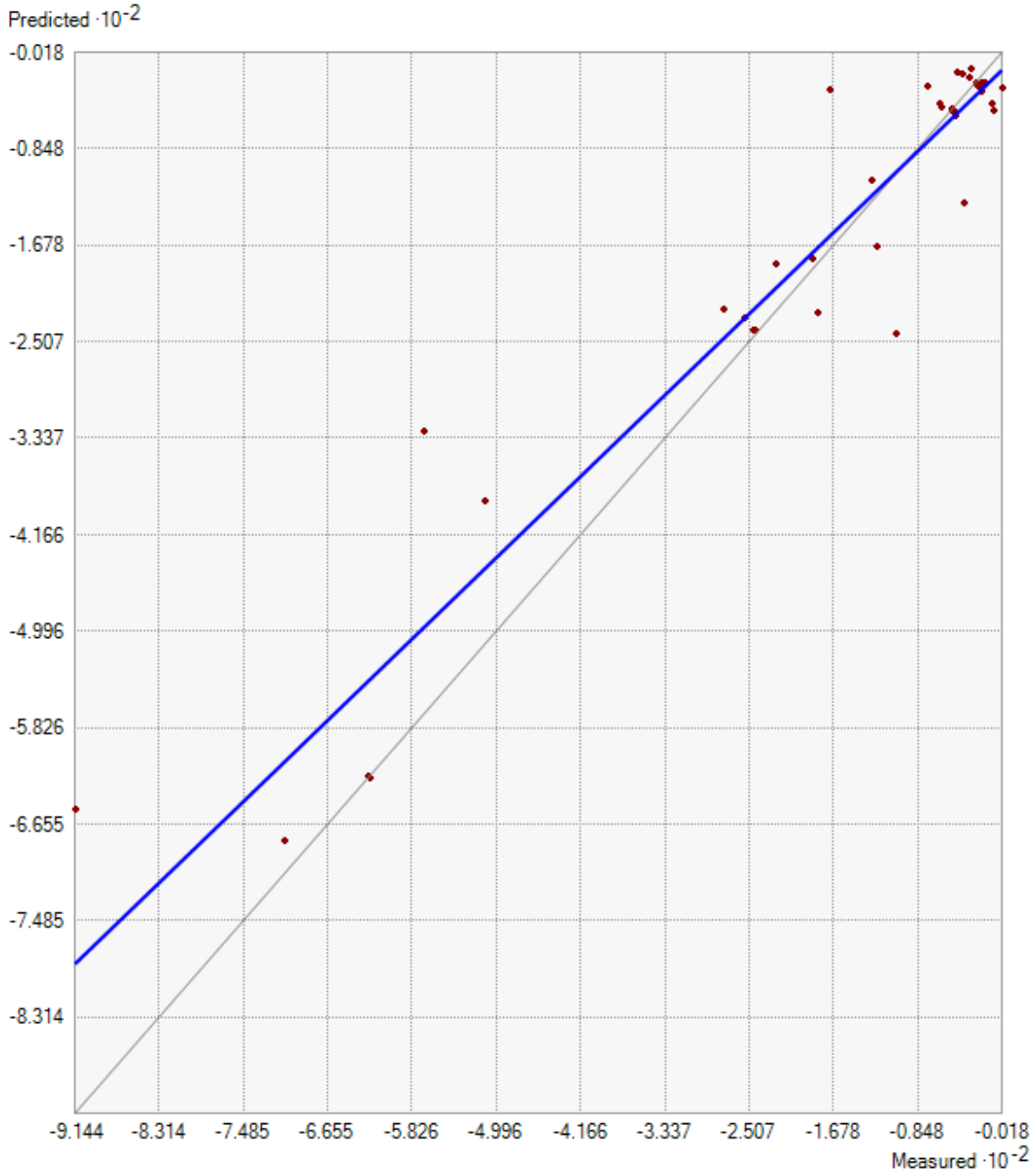

Regression function: 0.842341355094857 * x + -15.6094517276762

Samples: 40

Mean 15.54794

RMSE: 72.32201

Appendix B. Interpolation Results: Potomac Aquifer

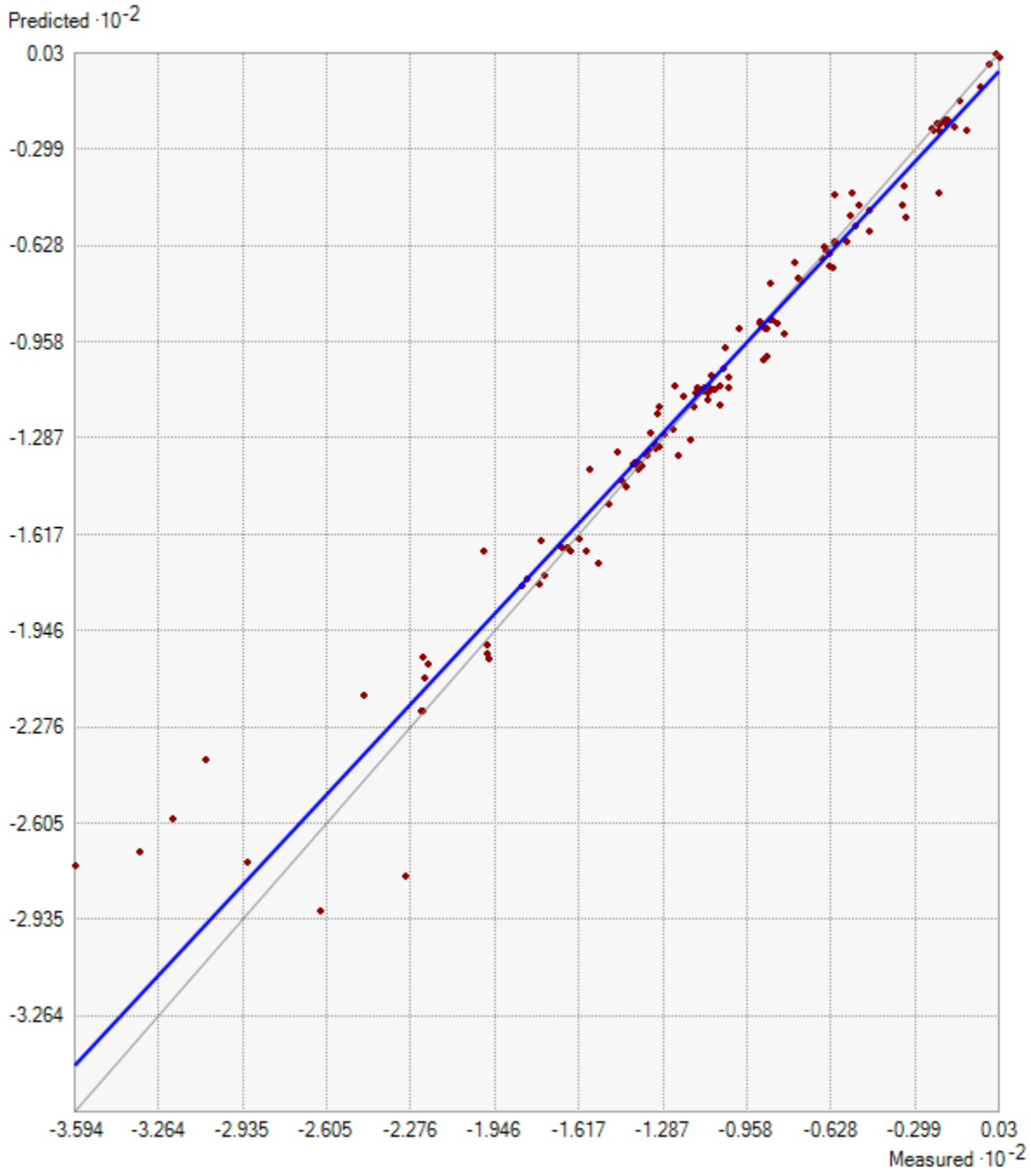

Regression function: 0.939215390432397 * x + -5.958618057116

Samples: 126

Mean 2.038808

RMSE: 15.75015

Appendix C. Interpolation Results: Potomac Confining Unit

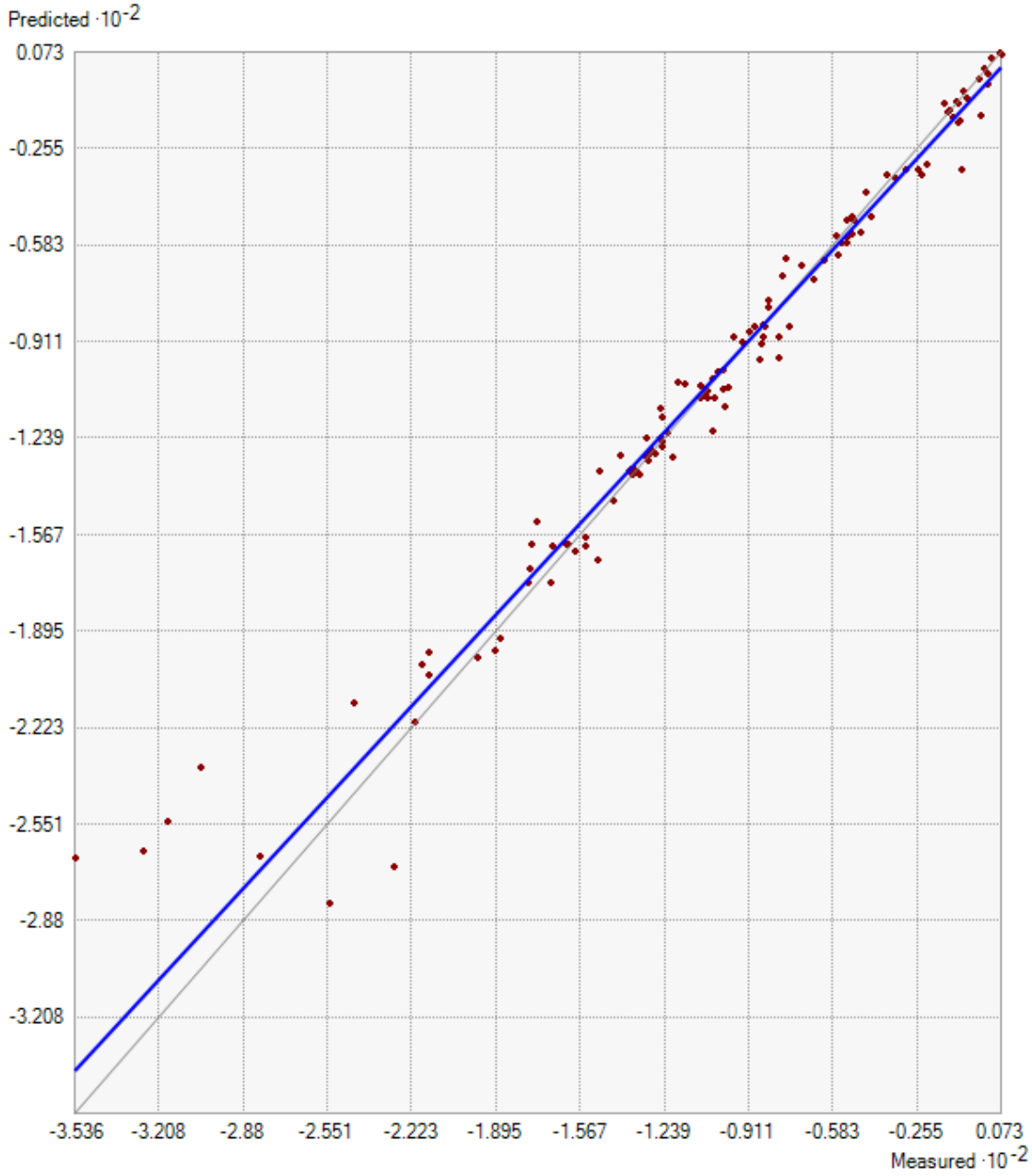

Regression function: 0.94537563207137 * x + -4.81692779895447

Samples: 127

Mean 2.193643

RMSE: 15.40932

Appendix D. Interpolation Results: Land Surface

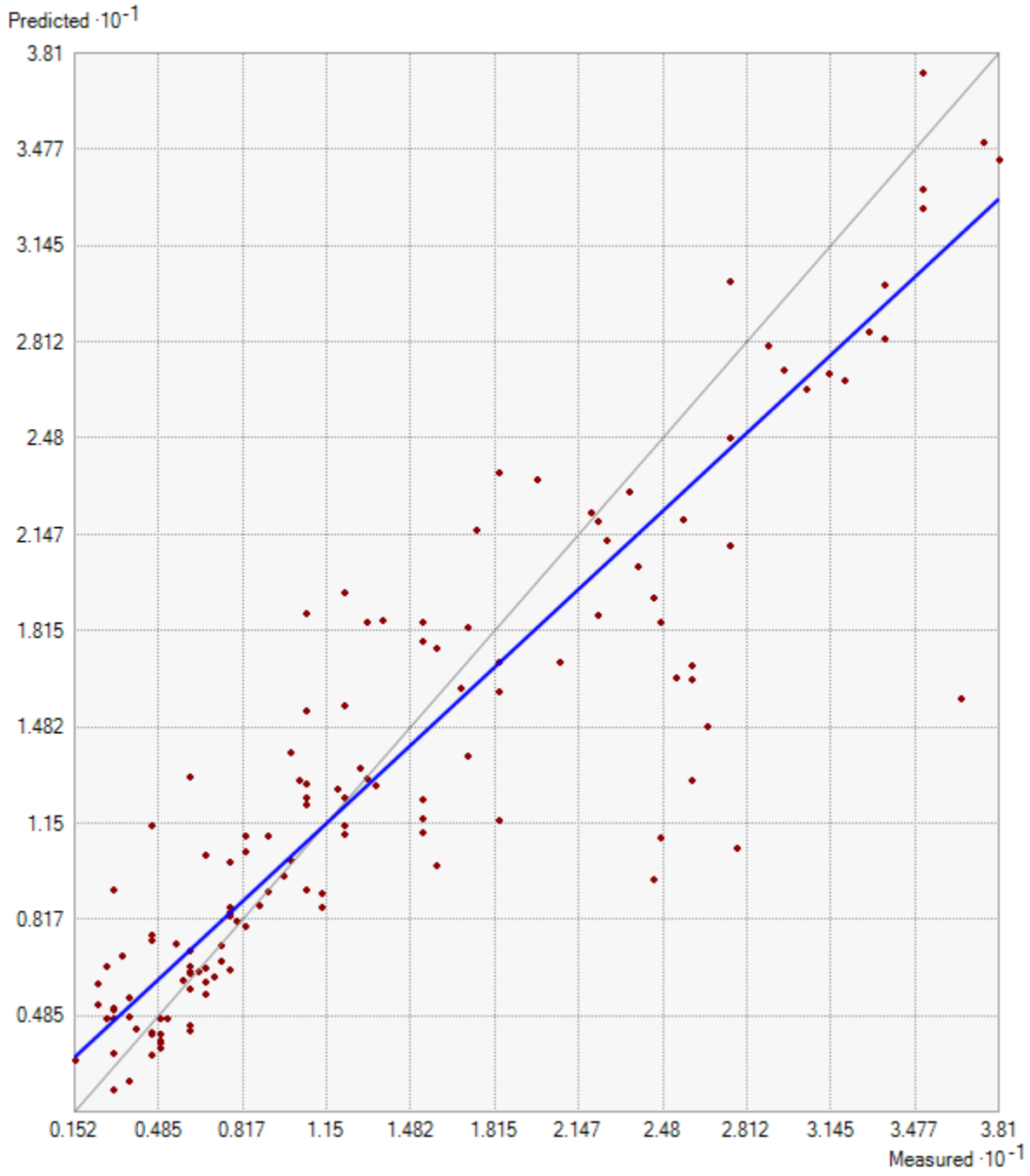

Regression function: 0.81063691777702 * x + 2.18148571495346

Samples: 137

Mean -.07346661

RMSE: 4.488759

Appendix E. Additional Estimated Damages

Table 30: Private Subsidence Damage from 10 years of Pumping

Pump Site	Private Subsidence Damage Lower Bound 10 years	Private Subsidence Damage Upper Bound 10 years
1	$1.81	$8.90
2	$2.40	$11.80
3	$6.59	$32.38
4	$4.91	$24.13
5	$12.93	$63.53
6	$7.69	$37.76
7	$274.26	$1,347.43
8	$385.48	$1,893.90
9	$136.93	$672.72
10	$1,507.60	$7,406.91

Table 31: Private Subsidence Damage from 50 years of Pumping

Pump Site	Private Subsidence Damage Lower Bound 50 years	Private Subsidence Damage Upper Bound 50 years
1	$1.92	$9.43
2	$2.55	$12.50
3	$6.98	$34.30
4	$5.20	$25.56
5	$13.70	$67.30
6	$8.15	$40.02
7	$290.51	$1,427.30
8	$408.51	$2,007.04
9	$145.06	$712.70
10	$1,597.38	$7,848.01

Table 32: Private Subsidence Damage from 100 years of Pumping

Pump Site	Private Subsidence Damage Lower Bound 100 years	Private Subsidence Damage Upper Bound 100 years
1	$1.97	$9.66
2	$2.61	$12.81
3	$7.15	$35.13
4	$5.33	$26.17
5	$14.03	$68.92
6	$8.34	$40.99
7	$297.51	$1,461.68
8	$418.43	$2,055.78
9	$148.57	$729.92

10	$1,636.05	$8,037.99

Table 33: Total Subsidence Damage from 10 years of Pumping

Pump Site	Total Subsidence Damage Lower Bound 10 years	Total Subsidence Damage Upper Bound 10 years
1	$447,234.84	$2,197,284.23
2	$592,961.11	$2,913,243.69
3	$699,853.57	$3,438,411.01
4	$751,465.69	$3,691,983.61
5	$912,523.89	$4,483,269.54
6	$1,019,118.95	$5,006,975.73
7	$1,218,324.90	$5,985,683.20
8	$1,276,230.59	$6,270,176.38
9	$1,285,310.76	$6,314,787.63
10	$1,477,100.40	$7,257,058.49

Table 34: Total Subsidence Damage from 50 years of Pumping

Pump Site	Total Subsidence Damage Lower Bound 50 years	Total Subsidence Damage Upper Bound 50 years
1	$860,426.46	$4,227,312.60
2	$1,006,144.64	$4,943,232.34
3	$1,113,032.62	$5,468,377.65
4	$1,164,635.19	$5,721,903.31
5	$1,325,686.08	$6,513,153.34
6	$1,432,276.97	$7,036,839.02
7	$1,631,457.00	$8,015,419.16
8	$1,689,366.25	$8,299,929.84
9	$1,698,450.48	$8,344,561.03
10	$1,890,215.22	$9,286,709.54

Table 35: Total Subsidence Damage from 100 years of Pumping

Pump Site	Total Subsidence Damage Lower Bound 100 years	Total Subsidence Damage Upper Bound 100 years
1	$1,038,370.79	$5,101,560.85
2	$1,184,085.48	$5,817,463.43
3	$1,290,971.52	$6,342,599.22
4	$1,342,569.97	$6,596,104.65
5	$1,503,617.71	$7,387,339.16
6	$1,610,206.79	$7,911,015.97
7	$1,909,375.64	$8,889,541.19
8	$1,867,286.42	$9,174,059.38
9	$1,876,372.40	$9,218,699.18

10	$2,068,126.39	$10,160,797.99

Table 36: External Damages from Increased Pumping Height

Pump Site	External Pumping Damages 10 years	External Pumping Damages 50 years	External Pumping Damages 100 years
1	$28,699,120.00	$48,758,940.00	$57,398,240.00
2	$28,699,110.00	$48,758,930.00	$57,398,220.00
3	$28,699,110.00	$48,758,920.00	$57,398,210.00
4	$28,699,100.00	$48,758,900.00	$57,398,190.00
5	$28,699,070.00	$48,758,850.00	$57,398,130.00
6	$28,699,060.00	$48,758,840.00	$57,398,110.00
7	$28,698,450.00	$48,757,800.00	$57,396,900.00
8	$28,697,390.00	$48,756,000.00	$57,394,770.00
9	$28,698,560.00	$48,757,990.00	$57,397,120.00
10	$28,696,100.00	$48,753,810.00	$57,392,200.00

Table 37: Private Damages from Increased Pumping Height

Pump Site	Private Pumping Damages 10 years	Private Pumping Damages 50 years	Private Pumping Damages 100 years
1	$17.42	$29.59	$34.83
2	$24.28	$41.24	$48.55
3	$30.07	$51.08	$60.13
4	$40.18	$68.26	$80.35
5	$70.23	$119.32	$140.46
6	$79.88	$135.72	$159.76
7	$688.02	$1,168.92	$1,376.04
8	$1,749.02	$2,971.53	$3,498.04
9	$575.32	$977.45	$1,150.64
10	$3,036.40	$5,157.05	$6,070.79

Appendix F. Linear Programming Model

```
SET       N Damage Tracts /1*47748 /
          M Distances from pumping /D_22327, D_8432, D_7126, D_26559, D_33726,
              D_35584, D_41761, D_59742, D_46777, D_52654 /
          P AQ Parameters  /OID, cthick, pum, FZ, Elev, DisToWater, PctSlope, Forest,
              Water, Shrub, Wetland, PctArea, Homes, Num_Homes, Class_1, Class_2,
              water_pcpd /
          t year /1*10/;

table AQC(N,P) 'aquifer characteristics'
$ondelim
$include Cells_Chara_17_Mar_2.csv
$offdelim

table DIST(N,M) 'distance between tracts originally used Distance10_17_Mar_1 but the
results kept showing OID'
$ondelim
$include Distance10_17_Mar_3.csv
$offdelim

display AQC, DIST;

** SOLVING THE THEIS EQUATION **************************

scalars  pump          pumping rate (cfs)(1 Mgal per day) /1.54722865/
      tran          aquifer transmissivity (sq ft per day) /10000/
      st           storativity /0.0002/;

parameters
      day(t)        day
      u(N,M,t)      Theis parameter by tract and year
      w(N,M,t)      Theis parameter by tract and year
      ddf(N,M,t)    drawdown by tract and year (ft)
      ddm(N,M,t)    drawdown by tract and year (m);

day(t) =  365*ord(t);

u(N,M,t) = (sqr(DIST(N,M))*st)/(4*tran*day(t));
w(N,M,t) =  -0.9793 * log(u(N,M,t)) - 0.2722;
ddf(N,M,t) = (pump*w(N,M,t))/(12.57*(tran/86400));
ddm(N,M,t) = ddf(N,M,t)*0.3048;

display ddm;
```

```
** SOLVING FOR SUBSIDENCE ***********************************************

scalars
        fd          fluid density /1000/
        g           gravity /9.81/
        c           compressibility /0.0000001/;

parameters
        sub(N,M,t)      subsidence;

sub(N,M,t) = fd*g*ddm(N,M,t)*AQC(N,"cthick")*c;

display sub;


**SOLVING FOR COSTS*************************************

parameters
        mcelec          marginal cost elec /0.05497/
        psi             equivalent psi /29.964/
        ppeff           pumping plant eff /.6247/
        r               discount rate /.03125/
        lift(N,M,t)     pumping lift final period
        pc(N,M,t)       power consumption kwh per 10000m3
        mc(N,M,t)       cost $per 10000m3
        mc2(N,M)        Difference in cost from year 1 to year 10
        inccost(N,M)    Increse in cost from pumping Chaing pg 470 infinite time series
converges to Cost divided by discount rate
        mec(M)          marginal external cost of pumping in tract N
        mpc(M)          marginal private cost of pumping in tract N;

lift(N,M,t) = AQC(N,"pum")+ddm(N,M,t)-sub(N,M,t);
pc(N,M,t) = (((psi*2.31+((21/20)*lift(N,M,t))/0.3048))*1.02/(ppeff)*(8.11));
mc(N,M,t) = pc(N,M,t)*mcelec;
mc2(N,M) = mc(N,M,"10")-mc(N,M,"1");
inccost(N,M) = (mc2(N,M)*AQC(N,"water_pcpd"))/r;
display lift, pc, mc, mc2, inccost;

mec(M) = sum(N$(ord(M) ne ord(N)), inccost(N,M));
mpc(M) = sum(N$(ord(M) eq ord(N)), inccost(N,M));
display mec, mpc;

**IMPORTING LOGIT MODEL DUMMY ONLY FOR ELEVATION CLASS********
```

Scalars

B1_1	Beta 1 elev	/-0.291182/
B2_1	Beta 2 pctslope	/0.9165991/
B3_1	Beta 3 distowater	/0.0000128/
B4_1	Beta 4 forest	/-.4131278/
B5_1	Beta 5 water	/0.8978904/
B6_1	Beta 6 shrub	/-0.548274/
B7_1	Beta 7 wetland	/0.9323832/
B8_1	Beta 8 class_1	/-1.590992/
B9_1	Beta 9 class_2	/-0.02281/
CON1	Constant	/2.036011/

Parameters

NewElev1(N,M,t)	Elevation after yr 10 subsidence
Logit1_1(N)	Logit model
Odds1_1(N)	Convert Logit to odds
Prob1_1(N)	Convert odds to probability
Logit1_2(N,M,t)	Logit after SUB
Odds1_2(N,M,t)	Odds after SUB
Prob1_2(N,M,t)	Prob after SUB
Change_Prob1(N,M,t)	Change in probability;

```
NewElev1(N,M,"10") = AQC(N,"Elev")-sub(N,M,"10");
Logit1_1(N) =
(B1_1*AQC(N,"Elev"))+(B2_1*AQC(N,"PctSlope"))+(B3_1*AQC(N,"DisToWater"))+(B
4_1*AQC(N,"Forest"))+(B5_1*AQC(N,"Water"))+(B6_1*AQC(N,"Shrub"))+(B7_1*AQC
(N,"Wetland"))+(B8_1*AQC(N,"class_1"))+(B9_1*AQC(N,"class_2"))+CON1;
Odds1_1(N) = exp(Logit1_1(N));
Prob1_1(N) = Odds1_1(N)/(1+Odds1_1(N));

Logit1_2(N,M,t) =
(B1_1*NewElev1(N,M,"10"))+(B2_1*AQC(N,"PctSlope"))+(B3_1*AQC(N,"DisToWater")
)+(B4_1*AQC(N,"Forest"))+(B5_1*AQC(N,"Water"))+(B6_1*AQC(N,"Shrub"))+(B7_1*
AQC(N,"Wetland"))+(B8_1*AQC(N,"class_1"))+(B9_1*AQC(N,"class_2"))+CON1;
Odds1_2(N,M,t) = exp(Logit1_2(N,M,"10"));
Prob1_2(N,M,t) = Odds1_2(N,M,"10")/(1+Odds1_2(N,M,"10"));

Change_Prob1(N,M,t) = Prob1_2(N,M,"10")-Prob1_1(N);

display Logit1_1, Odds1_1, Prob1_1, Logit1_2, Odds1_2, Prob1_2, Change_Prob1;

**Damages**********
Scalars
    Loss    Expected Loss (2.3-11.3)(7.8) /.023/
```

```
Parameters
      Damage1(N,M,t)      Expected Damages
      extdamage(M)        External damages from subsidence
      privatedamage(M)    Private damages from subsidence;

Damage1(N,M,t) =
Change_Prob1(N,M,"10")*AQC(N,"Homes")*AQC(N,"Num_Homes")*AQC(N,"PctArea
")*Loss;

extdamage(M) = sum(N$(ord(M) ne ord(N)), Damage1(N,M,"10"));
privatedamage(M) = sum(N$(ord(M) eq ord(N)), Damage1(N,M,"10"));

display Damage1, extdamage, privatedamage;

**EXPORTING TO TXT**************************

FILE    IOUT /S_22327_Mar_21.TXT/
PUT     IOUT;
PUT     'SUB ' //;
LOOP(N, Put SUB(N,"D_22327","10"):8:4/);

FILE    IOUT2 /S_8432_Mar_21.TXT/
PUT     IOUT2;
PUT     'SUB' //;
LOOP(N, Put SUB(N,"D_8432","10"):8:4/);

FILE    IOUT3 /S_7126_Mar_21.TXT/
PUT     IOUT3;
PUT     'SUB' //;
LOOP(N, Put SUB(N,"D_7126","10"):8:4/);

FILE    IOUT4 /S_26559_Mar_21.TXT/
PUT     IOUT4;
PUT     'SUB' //;
LOOP(N, Put SUB(N,"D_26559","10"):8:4/);

FILE    IOUT5 /S_33726_Mar_21.TXT/
PUT     IOUT5;
PUT     'SUB' //;
LOOP(N, Put SUB(N,"D_33726","10"):8:4/);

FILE    IOUT6 /S_35584_Mar_21.TXT/
PUT     IOUT6;
PUT     'SUB' //;
LOOP(N, Put SUB(N,"D_35584","10"):8:4/);
```

```
FILE    IOUT7 /S_41761_Mar_21.TXT/
PUT     IOUT7;
PUT     'SUB' //;
LOOP(N, Put SUB(N,"D_41761","10"):8:4/);

FILE    IOUT8 /S_59742_Mar_21.TXT/
PUT     IOUT8;
PUT     'SUB ' //;
LOOP(N, Put SUB(N,"D_59742","10"):8:4/);

FILE    IOUT9 /S_46777_Mar_21.TXT/
PUT     IOUT9;
PUT     'SUB ' //;
LOOP(N, Put SUB(N,"D_46777","10"):8:4/);

FILE    IOUT10 /S_52654_Mar_21.TXT/
PUT     IOUT10;
PUT     'SUB ' //;
LOOP(N, PUT,SUB(N,"D_52654","10"):8:4/);
```

References

Alanis, Leon F. Gay. 2009. Measuring Energy Efficiency of Water Utilities. Master's Thesis, Virginia Polytechnic Institute and State University Blacksburg, Virginia.

Bartosova, Alena, David Clark, Vladimir Novotny, and Kyra. S. Taylor. 2000. Using GIS to Evaluate the Effects of Flood Risk on Residential Property Values. *EPA Conference* 1-35.

Beron, Kurt J., James C. Murdoch, Mark A. Thayer, and Wim P.M. Vijverberg. 1997. An Analysis of the Housing Market before and after the 1989 Loma Prieta Earthquake. *Land Economics* 73.1 (February): 101-113.

Bin, Okmyung, Jaimie Brown Kruse, and Craig E. Landry. 2008. Flood Hazards, Insurance Rates, and Amenities: Evidence from the Coastal Housing Market. *The Journal of Risk and Insurance* 75.1 (March): 63-82.

Bin, Okmyung, Thomas W. Crawford, Jamie B. Kruse, and Craig E. Landry. 2008. "Viewscapes and Flood Hazard: Coastal Housing Markey Response to Amenities and Risk." *Land Economics* 84.3 (August): 434-448.

Bin, Okmyung, and Stephen Polasky. 2004. Effects of Flood Hazards on Property Values: Evidence Before and After Hurricane Floyd. *Land Economics* 80.4 (November): 490-500.

Bouwer, Herman. 2002. Artificial Recharge of Groundwater: Hydrogeology and Engineering. *Hydrogeology Journal* 10 (January): 121-142.

Boxall, Bettina. 2015. Another toll of the drought: Land is sinking fast in San Joaquin Valley, study shows. *LA Times*. 19 August.

Brozovic, Nicholas, David Sunding, and David Zilberman. 2006. Optimal Management of Groundwater over Space and Time. *Frontiers in Water Resource Economics* New York: Springer.

Chiang, Alpha C. 1984. *Fundamental Methods of Mathematical Economics.* 3rd ed. Singapore: McGraw-Hill Inc.

Chivers, James, and Nicholas E. Flores. 2002. Market Failure in Information: The National Flood Insurance Program. *Land Economics* 78.4 (November): 515-521.

Chesapeake Bay Program. 2011. "State of the Chesapeake Bay Program: Summary Report to the Chesapeake Executive Council." Available online at http://www.chesapeakebay.net/library. Accessed March 2015.

Coase, R.H. 1960. "The Problem of Social Cost," *Journal of Law and Economics* 3 (October): 1-44.

Cobourn, Kelly M. Externalities and Simultaneity in Surface Water-Groundwater Systems: Challenges for Water Rights Institutions, in press, American Journal of Agricultural Economics.

Contor, Bryce A., Garth Taylor, and Greg L. Moore. 2008. IRRIGATION DEMAND CALCULATOR: Spreadsheet Tool for Estimating Economic Demand for Irrigation Water. *Idaho Water Resources Research Institute Technical Report 200803*: 47.

Deming, David. 2002. *Introduction to Hydrogeology.* 1st ed. Boston: McGraw-Hill Inc.

Eggleston, Jack, and Jason Pope. 2013. Land Subsidence and Relative Sea-Level Rise in the Southern Chesapeake Bay Region. U.S. Geological Survey Circular 1392.

Faisal, Islam M., Robert A. Young, and James W. Warner. 1994. An Integrated Economic Hydrologic Model for Groundwater Basin Management. Colorado Water Resources Research Institute Completion Report No. 186.

Federal Energy Regulatory Commission. 2013. *PJM Annual Average Bilateral Prices*. http://www.ferc.gov/market-oversight/mkt-electric/pjm/elec-pjm-yr-pr.pdf Accessed 15 Oct. 2015.

Feinerman, Eli, and Keith C. Knapp. 1983. Benefits from Groundwater Management: Magnitude, Sensitivity, and Distribution. *American Journal of Agriculture Economics* 65 (December): 703-710.

Freeze, R.A., and John A. Cherry. 1979. *Groundwater*. Englewood Cliffs, NJ: Prentice-Hall.

Field, Barry C. 2005. *Natural Resource Economics: An Introduction*. Long Grove, IL: Waveland Press.

Galloway, Devon L., and Thomas J. Burbey. 2011. Review: Regional Land Subsidence Accompanying Groundwater Extraction. *Hydrogeology Journal* 19.8 (December): 1459-1486.

Galloway, Devon L., David R. Jones, and S.E. Ingebritsen. 1999. Land Subsidence in the United States. U.S. Geological Survey Circular 1182.

Gisser, Micha. 1983. Groundwater: Focusing on the Real Issues. *The Journal of Political Economy* 91.6 (December): 1001-1027.

Gisser, Micha, and David A. Sanchez. 1980. Competition Versus Optimal Control in Groundwater Pumping. *Water Resources Research* 16.4 (August): 638-642.

Goodell, S.A. 1988. Water use on the Snake River plain, Idaho and eastern Oregon. U.S. Geological Survey Professional Paper 1408-E.

Hallstrom, Daniel G., and V.K. Smith. 2005. Market Responses to Hurricanes, *Journal of Environmental Economics and Management* 50.3 (November): 541-561.

"Index of FEMA/Risk_MAP/NFHL" last Modified May 4 2016. https://data.femadata.com/FIMA/Risk_MAP/NFHL/.

Job, Charles A. 2010. *Groundwater Economics*. Boston: CRC Press.

Katic, Pamela G. 2011. Three Essays on the Economics of Groundwater Extraction. PhD Thesis, The Australian National University, Canberra, Australia.

Katic, Pamela G., and R.Q. Grafton. 2012. Economic and Spatial Modelling of Groundwater Extraction, *Hydrogeology Journal* 20.5 (August): 831-834.

Knapp, Keith, and Kenneth A. Baerenklau. 2006. Ground Water Quantity and Quality Management: Agricultural Production and Aquifer Salinization over Long Time Scales. *Journal of Agricultural and Resource Economics* 31.3 (December): 616-641

Kolstad, Charles D. 2011. *Intermediate Environmental Economics*, 2nd ed. New York: Oxford University Press.

Koundouri, Phoebe. 2004. Current Issues in the Economics of Groundwater Resource Management. *Journal of Economic Surveys* 18.5: 703-740.

Kumar, Awkash, Indrani Gupta, Jørgen Brandt, Rakesh Kumar Anil K. Dikshit, and Rashmi S. Patil. 2016. Air Quality Mapping Using GIS and Economic Evaluation of Health Impact for Mumbai City, India. *Journal of the Air and Waste Management Association* 66.5 (February): 470-481.

Kuwayama Yusuke, and Nicholas Brozovic. 2012. Analytical Hydrologic Models and the Design of Policy Instruments for Groundwater-Quality Management, *Hydrogeology Journal* 20.5 (August): 957-972.

Kuwayama, Yusuke, and Nicholas Brozovic. 2013. The Regulation of a Spatially Heterogeneous Externality: Tradable Groundwater Permits to Protect Streams. *Journal of Environmental Economics and Management* 66.2 (September): 364-382.

Landry, Craig E., Andrew G. Keeler, and Warren Kriesel. 2003. An Economic Evaluation of Beach Erosion Management Alternatives. *Marine Resource Economics* 18: 105-127.

Lant, Christopher L., Steven E. Kraft, Jeffery Beaulieu, David Bennett, Timothy Luftos, John Nicklow. 2005. Using GIS-Based Ecological-Economic Modeling to Evaluate Policies Affecting Agricultural Watersheds. *Ecological Economics*, 55.4 (December): 467-484.

Lee, Kun C., Cameron Short, and Earl O. Heady. 1981. Optimal Groundwater Mining in the Ogallala Aquifer: Estimation of Economic Losses and Excessive Depletion Due to Commonality. Center for Agriculture and Rural Development, Iowa State University, Iowa, USA.

MacDonald, Don N., Harry L. White, Paul M. Taube, and William L. Huth. 1990. Flood Hazard Pricing and Insurance Premium Differentials: Evidence from the Housing Market. *The Journal of Risk and Insurance* 57.4 (December): 654-663.

Masterson, John P., Jason P. Pope, Jack Monti Jr., Mark R. Nardi, Jason F. Finkelstein, and Kurt J. McCoy. 2015. Hydrogeology and Hydrologic Conditions of the Northern Atlantic Coastal Plain Aquifer System from Long Island, New York, to North Carolina. U.S. Geological Survey Scientific Investigations Report 2013-5133.

Maupin, Molly A., Joan F. Kenny, Susan S. Hutson, John K. Lovelace, Nancy L. Barber, and Kristin S. Linsey. 2014. Estimated use of water in the United States in 2010. U.S. Geological Survey Circular 1405.

McClusky, Jill J., and Gordon C. Rausser, 2001. Estimation of Perceived Risk and Its Effects on Property Values. *Land Economics* 77.1 (February): 42-55.

McFarlane, Benjamin J. 2012. Climate Change in Hampton Roads- Phase III- Sea Level Rise in Hampton Roads, Virginia. Hampton Roads Planning District Commission Report PEP12-06.

McFarland, E.R. 2013. Sediment Distribution and Hydrologic Conditions of the Potomac Aquifer in Virginia and Parts of Maryland and North Carolina. U.S. Geological Survey Scientific Investigations Report 2013-5116.

McFarland, E. R., and T. S. Bruce. 2006. The Virginia Coastal Plain Hydrogeologic Framework. U.S. Geological Survey Professional Paper 1731.

Michael, Jeffrey A. 2007. Episodic flooding and the cost of sea-level rise. *Ecological Economics* 63.1 (June):149-159.

Millennium Ecosystem Assessment (MEA). 2003. "Ecosystems and Human Well-Being: A framework for Assessment." *n. pag*. Available online at http://www.millenniumassessment.org/en/Framework.html. Accessed March 2015.

Nicholson, Walter, and Christopher Snyder. 2012. *Microeconomic Theory: Basic Principles and Extensions.*11th ed. Andover, UK: Cengage Learning.

Pfeiffer, Lisa, and C.-Y. Cynthia Lin. 2014. Does Efficient Irrigation Technology Lead to Reduced Groundwater Extraction? Empirical Evidence. *Journal of Environmental Economics and Management* 67.2 (March): 189-208.

Poland, Joseph F. 1984. Guidebook to Studies of Land Subsidence due to Ground-Water Withdrawal. International Hydrological Programme Working Group 8.4.

Pigou, Arthur C. 1938. *The Economics of Welfare*. 4th ed. London: Macmillan and Co.

Provencher, Bill, and Oscar Burt. 1993. The Externalities Associated with the Common Property Exploitation of Groundwater. *Journal of Environmental Economics and Management* 24.2 (March): 139-158.

Rosen, Sherwin. 1974. Hedonic Prices and Implicit Markets: Product Differentiation in Pure Competition. *Journal of Political Economy* 82.1 (January): 34-55.

Roumasset, James A., and Christopher A. Wada. 2010. Optimal and Sustainable Groundwater Extraction. *Sustainability* 2 (August): 2676-2685.

Theis, Charles V. 1938. The Significance and Nature of the Cone of Depression in Ground-Water Bodies. *Economic Geology* 33.8 (December): 889-902.

Tsur, Yacov. 1990. The Stabilization Role of Groundwater When Surface Water Supplies are Uncertain: The Implications for Groundwater Development. *Water Resources Research* 26.5 (May): 811-818.

Tsur, Yacov, and T. Graham-Tomasi. 1991. The Buffer of Groundwater with Stochastic Surface Water Supplies. *Journal of Environmental Economic Management* 21: 811-818.

U.S. Census Bureau, Annual Estimate of the Resident Population: April 1, 2010 to July 1, 2014. Accessed 1 Mar, 2016. http://factfinder.census.gov/faces/tableservices/jsf/pages/productview.xhtml?src=bkmk.

U.S. Department of Agriculture, Rate for Federal Water Projects: NRCS Economics. Accessed 5 April, 2016. http://www.nrcs.usda.gov/wps/portal/nrcs/detail/national/technical/econ/prices/?cid=nrcs143_009685.

Vecchia, Aldo V. 2008. Climate simulation and flood risk analysis for 2008-40 for Devils Lake, North Dakota. US Department of the Interior, US Geological Survey Scientific Investigations Report 2008-5011.

"Wolfram," last modified May 3, 2016. http://mathworld.wolfram.com/VoronoiDiagram.html.

Wooldridge, Jeffery M. 2013. *Introductory Econometrics: A Modern Approach*. 5th ed. Mason, OH: South-Western Cengage Learning.

Zervas, Chris. 2009. Sea Level Variations of the United States, 1854-2006. National Oceanic and Atmospheric Administration Technical Report NOS CO-OPS 053.